

**Zeitschrift:** Eclogae Geologicae Helvetiae  
**Herausgeber:** Schweizerische Geologische Gesellschaft  
**Band:** 71 (1978)  
**Heft:** 3

**Artikel:** Deformation in the Theodul-Rothorn zone (Zermatt, Switzerland)  
**Autor:** Wilson, Christopher J.L.  
**DOI:** <https://doi.org/10.5169/seals-164744>

### **Nutzungsbedingungen**

Die ETH-Bibliothek ist die Anbieterin der digitalisierten Zeitschriften auf E-Periodica. Sie besitzt keine Urheberrechte an den Zeitschriften und ist nicht verantwortlich für deren Inhalte. Die Rechte liegen in der Regel bei den Herausgebern beziehungsweise den externen Rechteinhabern. Das Veröffentlichen von Bildern in Print- und Online-Publikationen sowie auf Social Media-Kanälen oder Webseiten ist nur mit vorheriger Genehmigung der Rechteinhaber erlaubt. [Mehr erfahren](#)

### **Conditions d'utilisation**

L'ETH Library est le fournisseur des revues numérisées. Elle ne détient aucun droit d'auteur sur les revues et n'est pas responsable de leur contenu. En règle générale, les droits sont détenus par les éditeurs ou les détenteurs de droits externes. La reproduction d'images dans des publications imprimées ou en ligne ainsi que sur des canaux de médias sociaux ou des sites web n'est autorisée qu'avec l'accord préalable des détenteurs des droits. [En savoir plus](#)

### **Terms of use**

The ETH Library is the provider of the digitised journals. It does not own any copyrights to the journals and is not responsible for their content. The rights usually lie with the publishers or the external rights holders. Publishing images in print and online publications, as well as on social media channels or websites, is only permitted with the prior consent of the rights holders. [Find out more](#)

**Download PDF:** 14.12.2025

**ETH-Bibliothek Zürich, E-Periodica, <https://www.e-periodica.ch>**

Eclogae geol. Helv.	Vol. 71/3	Pages 517–549	18 figures in the text	Basle, November 1978
---------------------	-----------	---------------	---------------------------	----------------------

## Deformation in the Theodul–Rothorn Zone (Zermatt, Switzerland)

By CHRISTOPHER J. L. WILSON<sup>1)</sup>

### ABSTRACT

The Theodul–Rothorn Zone is a Mesozoic sedimentary sequence that forms part of a single major tectonic unit, the Combin Zone. The lithological and structural features in a small area of the Theodul–Rothorn Zone above Zermatt are described. It has suffered three main phases of Alpine deformation:

1. Early thrusting that is accompanied by the  $F_1$  folding phase and the nucleation of the metamorphic assemblages.
2. Intense folding ( $F_2$ ) and the formation of the Mischabel backfold and an accompanying foliation ( $S_2$ ). Shear zones develop subparallel to the  $S_2$  foliation planes and are confined notably to some lenticular marble units that are characterized by a fine mylonitic foliation; the shear zones parallel the lower limb of the Mischabel backfold.
3. Formation of subvertical kinks and brittle fracture features.

The nature, extent of deformation and thrusting associated with the first phase of deformation are difficult to establish as the sequence has been extensively modified by the  $F_2$  deformation phase. Most  $F_2$  folds have subhorizontal axial traces and the dominant layering and schistosity dip gently north-west.  $F_2$  fold axes plunge gently westward or to the north-west and appear to be parasitic to the Mischabel backfold. These folds are associated with a complex strain pattern, extensive flattening and variable deformation paths. The whole sequence is intersected by minor and major subhorizontal shear zones, which represent late thrusting, they parallel the pre-existing nappe boundaries and appear to be related to the  $F_2$  folding phase. These shear zones represent zones of brittle and intense plastic deformation, but are locally overprinted by solution effects and the later  $F_3$  deformation.

### ZUSAMMENFASSUNG

Die Theodul–Rothorn-Zone besteht aus einer Abfolge mesozoischer Sedimente und beteiligt sich am Aufbau einer grösseren tektonischen Einheit, der Combin-Zone. Die lithologischen und strukturellen Merkmale in einem kleinen Gebiet der Theodul–Rothorn-Zone oberhalb von Zermatt werden beschrieben. Man kann drei Phasen alpiner Verformung unterscheiden:

1. Frühe Überschiebung, begleitet von einer  $F_1$ -Faltungsphase und Bildung der metamorphen Paragenesen.
2. Intensive Faltung ( $F_2$ ) und Bildung der Mischabel-Rückfalte; ferner eine begleitende Kristallisationsschieferung ( $S_2$ ). Scherzonen entwickeln sich subparallel zu den  $S_2$ -Schieferungsflächen; sie sind bemerkenswerterweise auf einige linsenförmige Karbonat-Vorkommen beschränkt, gekennzeichnet durch ein feines mylonitisches Gefüge. Die Scherzonen verlaufen parallel zum liegenden Schenkel der Mischabel-Rückfalte.
3. Entstehung subvertikaler Knickungen (kinks) und spröde Bruchbildungen.

---

<sup>1)</sup> Department of Geology, School of Earth Sciences, University of Melbourne, Parkville, Victoria, 3052 (Australia).

Art und Ausmass der Verformung sowie der im Zusammenhang mit der ersten Deformationsphase erfolgte Zusammenschub sind schwierig festzustellen, da die Schichtfolge durch die  $F_2$ -Phase wesentlich verändert wurde. Die meisten  $F_2$ -Falten haben subhorizontale Achsenspuren, und die vorherrschende Schichtung bzw. Schieferung weist ein schwaches Einfallen nach Nordwesten auf. Die  $F_2$ -Faltachsen zeigen eine leichte Neigung gegen Westen oder Nordwesten und scheinen parasitär zur Mischabel-Rückfalte zu sein. Diese Falten sind assoziiert mit komplizierten Deformationserscheinungen, weiträumiger Plättung und unterschiedlichen Verformungsrichtungen. Die ganze Sequenz ist von subhorizontalen Neben- und Hauptscherzonen durchzogen, welche spätere Überschiebungen darstellen; sie laufen parallel zu den bereits bestehenden Deckengrenzen und scheinen mit der  $F_2$ -Faltungsphase zusammenzuhängen. Diese Scherzonen entsprechen Bereichen mit spröder und starker plastischer Deformation, sind aber örtlich von Auflösungserscheinungen und der späteren  $F_3$ -Verformung überprägt.

## CONTENTS

Introduction .....	518
Methods and scope of study .....	520
Distribution of lithologies .....	523
General .....	523
Trift Valley section .....	523
Zermatt section .....	526
Hubel section .....	528
Fold succession and geometry .....	529
Pre- $F_2$ deformation .....	529
$F_2$ deformation .....	530
Lineations .....	533
Shape characteristics of $F_2$ folds .....	533
Post- $F_2$ shear zones .....	537
$F_3$ deformation features .....	539
Macroscopic geometry .....	540
Conditions of metamorphism and microstructure .....	540
Relationship of Theodul-Rothorn Zone to Mischabel backfold .....	546
Conclusions .....	546
References .....	547

## Introduction

In the vicinity of Zermatt, Canton Valais (Fig. 1), a detailed picture of Alpine geology and its position in the regional structure of the central Pennine Alps has emerged since the pioneering interpretation of ARGAND (1911). The dominant structure in this region is the Mischabel backfold or "Mischabel-Rückfalte" (Fig. 2), and is one of a number of recumbent south-closing antiforms (MILNES 1974) observed in the Pennine Alps. This structure (Fig. 2) is formed where the cover and pre-Mesozoic core of the Grand St-Bernhard nappe are backfolded and apparently overturned onto the Mesozoic cover of the higher level Monte Rosa nappe (HEIM 1921, BEARTH 1967*a, b*). The Mesozoic envelope of the Monte Rosa nappe is composed mostly of ophiolites with thin, underlying Triassic quartz schists and carbonates; in the Mischabel region this envelope is also known as the Zone of Zermatt-Saas (BEARTH 1953). Both the Grand St-Bernhard and the Monte Rosa nappes are overlain by the Dent Blanche nappe; being subdivided into a lower unit, the Arolla Series, correlative with the Sesia-Lanzo Zone (CARRARO et al. 1970) and an upper tectonically emplaced unit, the Valpelline Series (CARRARO et al. 1970).

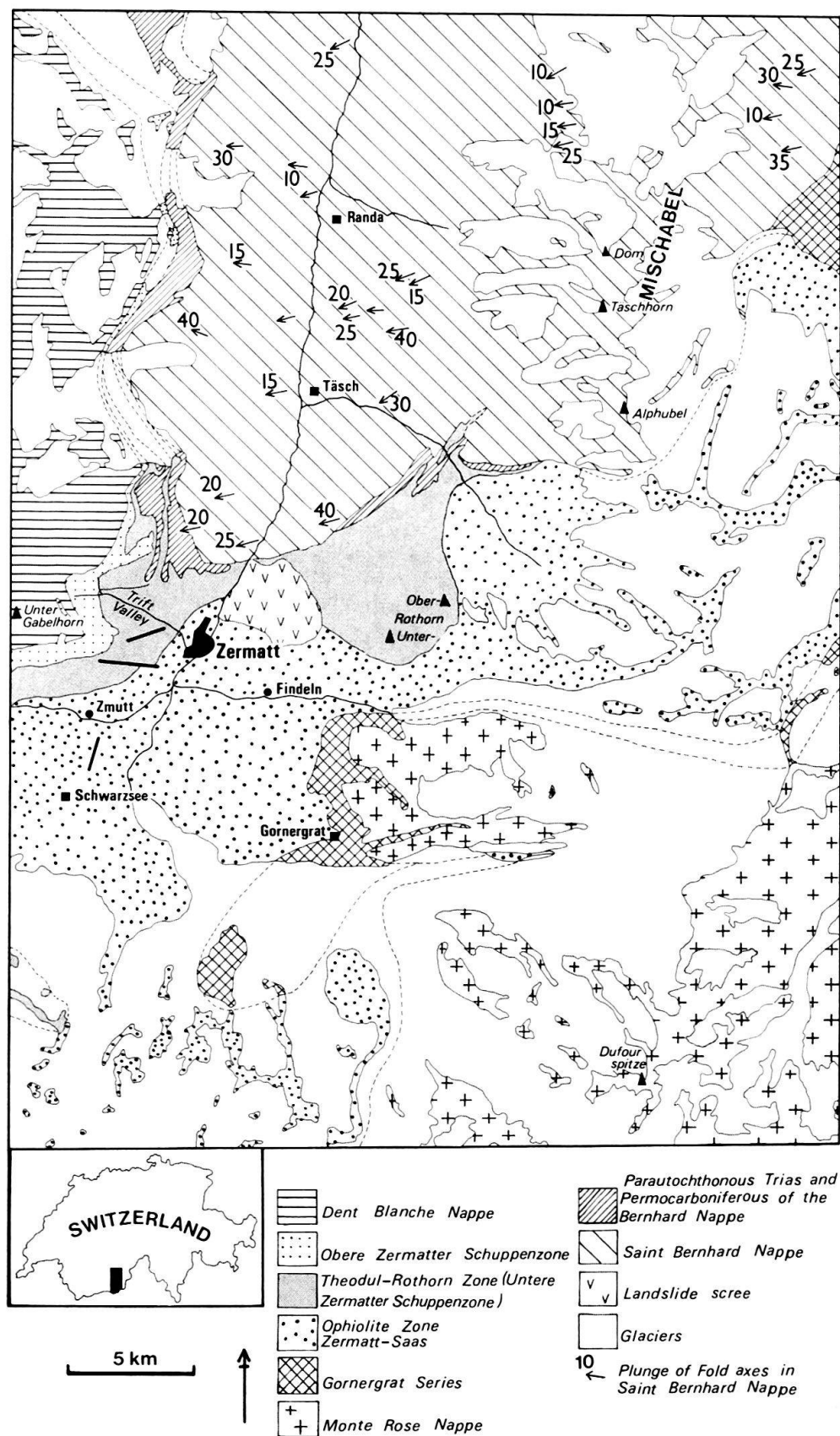


Fig. 1. Locality and geological sketch map (modified after BEARTH 1953, 1964) of Zermatt and surrounding areas, showing the plunge of the main portion of the Mischabel-Rückfalte in the St-Bernhard nappe.



The Dent Blanche nappe at Zermatt is directly superimposed on a Mesozoic sequence known as the higher (Obere) and lower (Untere) Zermatter Schuppenzone. This sequence, which is part of the Combin Zone (BEARTH 1976), separates the Dent Blanche nappe from the backfolded Bernhard–Monte Rosa nappes and Zermatt–Saas cover rocks. The Mischabel backfold plunges underneath the Dent Blanche nappe. However, the Dent Blanche nappe does not appear to have been affected by the folding responsible for the Mischabel backfold, a feature that has been noted by a number of workers.

### Methods and scope of study

This study is restricted to the Mesozoic sedimentary sequence that was called the Untere Zermatter Schuppenzone (BEARTH 1953) and later referred to as the Theodul–Rothorn Zone (BEARTH 1962) and is particularly concerned with the deformation within the quartzites, Bündnerschiefer (calcareous schists) (BEARTH 1976) and calcite–dolomite marbles. Mapping was done first on a horizontal plane at the scale of 1:10 000 and it was found that the lithological boundaries varied little from the positions already mapped by BEARTH (1953). Because of the strong relief in this area such a map gave little idea of the distribution of rock types or complexity of later folding. Instead photographs (essentially vertical sections) taken from the opposite sides of the valley were used; the scale of this mapping was approximately 1:2000. Special attention was placed on the minor structures in the Mesozoic rocks particularly the fold styles, orientation, and on their sequence of development. On the basis of this work three major Alpine deformations  $F_1$ ,  $F_2$  and  $F_3$  in order of their development were recognized with associated schistositys labelled  $S_1$ ,  $S_2$  and  $S_3$ .

Recumbent tight to isoclinal  $F_2$  folds are the dominant folding phase that deforms the Mesozoic rocks. The hinge lines of the folds plunge gently north-west, while the axial surfaces are subhorizontal. A penetrative schistosity lying parallel to the axial planes of the  $F_2$  folds is an important feature distinguishing them from folds related to other deformations. Few  $F_1$  minor folds were observed. However, the Mesozoic layers ( $S$ ) lie parallel to a schistosity which is being called an  $S_1$  schistosity, this being folded in the hinges of the  $F_2$  folds. The bedding  $S$  is defined on compositional differences as few sedimentary structures are preserved in the sequence.

The upper portion of the Theodul–Rothorn Zone (BEARTH 1962) is not described in this study nor are the ophiolites of the Zermatt–Saas Zone which have been adequately described by BEARTH (1967*a*). In the lower portion of the Theodul–Rothorn Zone one strongly deformed and recrystallized zone of sediments was mapped in detail (Fig. 3). This was the sequence exposed in the lower portion of the Trift Valley which extends north to Spiss and south-west in the direction of Zmutt at the foot of Unter Gabelhorn. The sequence was referred to by ARGAND (1909) as the “Groupe du Hubel” and characterized by “quartzites feuilletés avec lits subordonnés de calcaires dolomitiques et de prasinites”. As pointed out by GÜLLER (1947, p. 49) there is no prasinite in this section.

The number and thickness of different compositional layers within this zone varies considerably at different localities and it is often difficult to trace individual

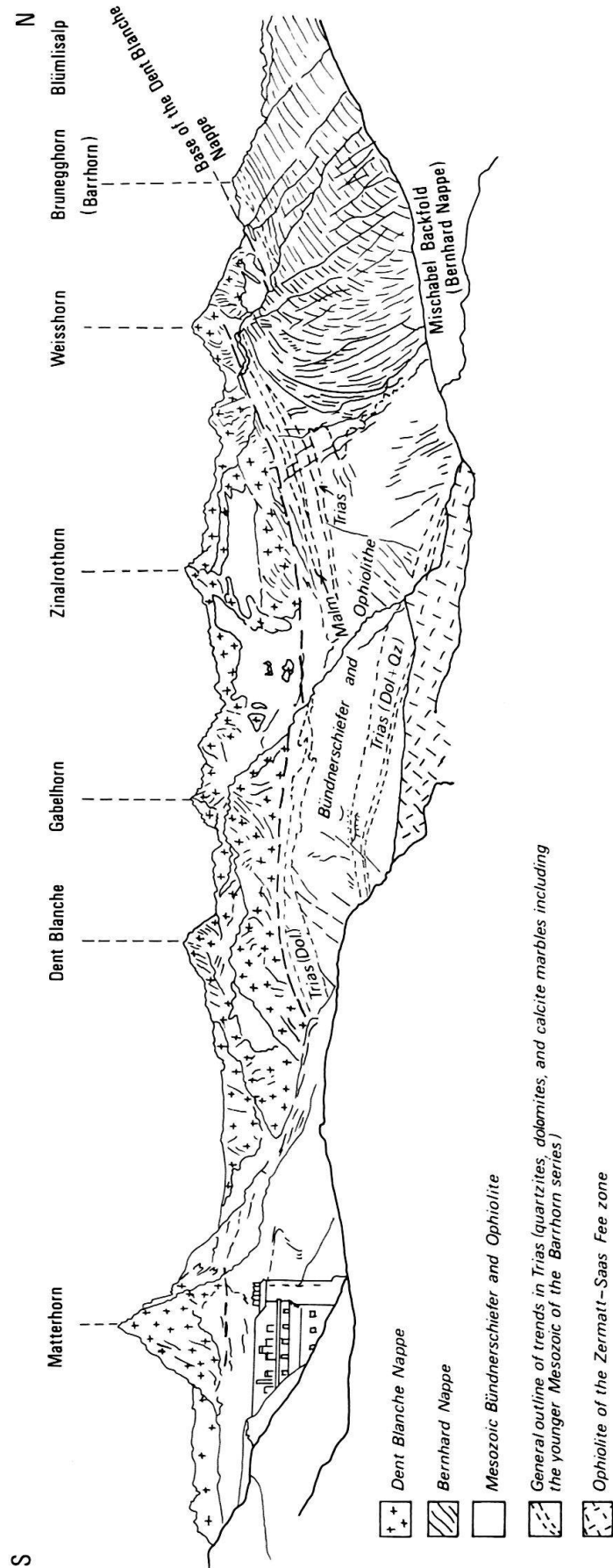


Fig. 2. Schematic view of the Zermatt region showing the Mischabel-Rückfalte in the St-Bernhard nappe (mainly after BEARTH 1967b).

units for any great distance along a cliff face. A few layers end in tight *V*-shaped forms or in a train of lenticular-shaped boudins; but others were traced for considerable distance only to be faulted out or disappear under scree cover. The sharp boundaries of the layers within this zone are parallel to the schistosity and also parallel to the contact of the overlying Bündnerschiefer and are apparently not folded with the underlying ophiolite sequence of the Zermatt-Saas Zone. One of the major problems in the area is to determine if the contacts represent unconformities or thrust contacts and whether these units are tectonically intercalated between the ophiolite sequence and the Bündnerschiefer.

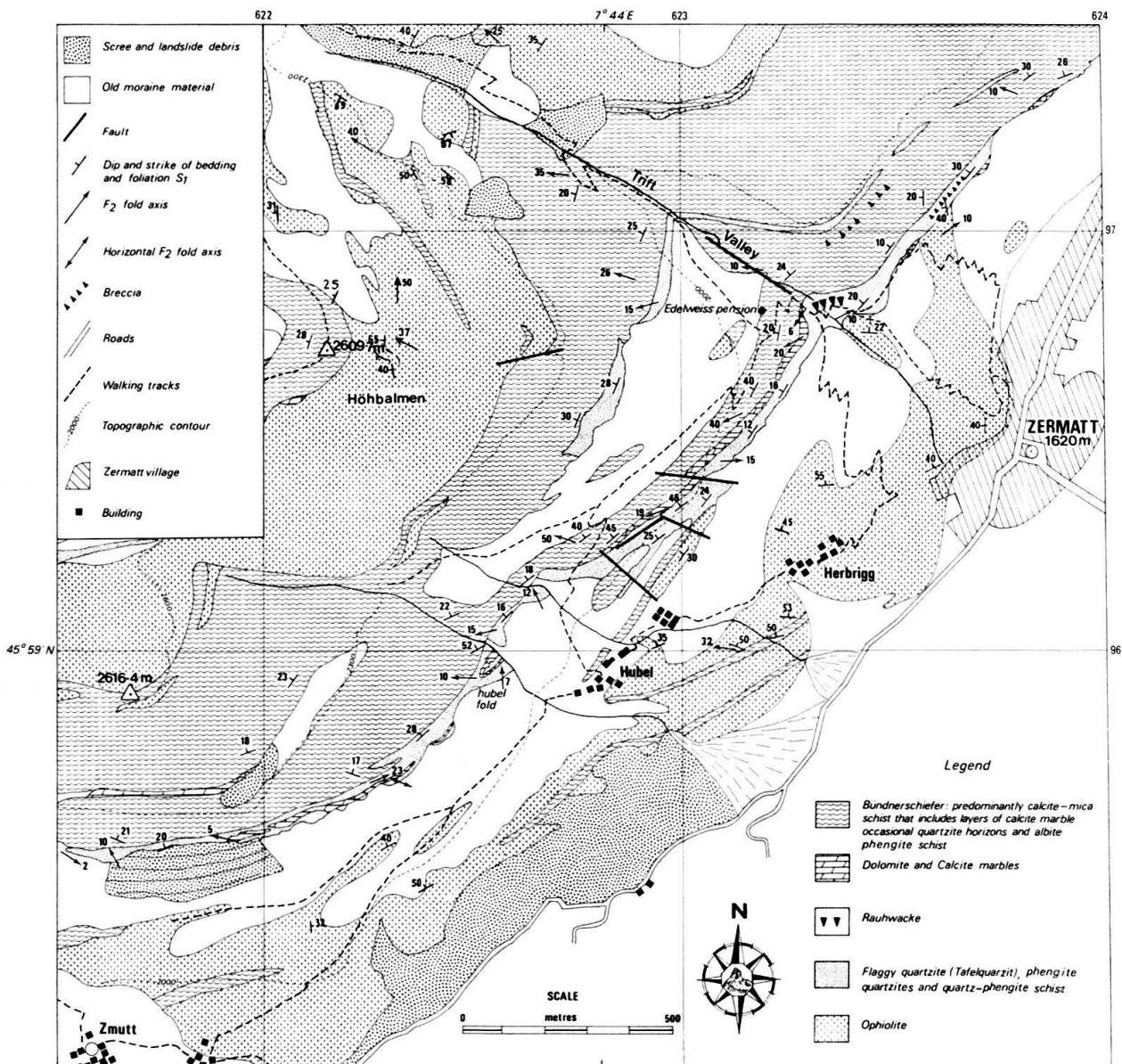


Fig. 3. Geological map of the Zmutt-Hubel-Trift Valley region west of Zermatt (modified after BEARTH 1953). The lower group of ophiolites belong to the ophiolite zone Zermatt-Saas. The Theodul-Rothorn Zone includes the quartzites, mica schist units, calcite-dolomite marbles, Bündnerschiefer and the upper ophiolite zone. The Obere Zermatter Schuppenzone begins with the second large Bündnerschiefer unit, a small portion of which is shown in the north-west corner of the map at Höhbalmen.

## Distribution of lithologies

### *General*

The thick and particularly prominent group of quartzites and quartz-phengite schist horizons intercalated with the marbles and calcareous schists can be followed from north of the Zermatt Bahnhof in a south-westerly direction to just north of Zmutt where they are concealed beneath scree (Fig. 4). At a number of localities along their outcrop these quartzites exhibit a symmetric repetition of rock types most of which can be traced into minor and major fold closures. The most prominent closure occurs at grid reference (coord.) 622.50/95.80 and will be referred to as the Hubel fold. The hinge zone of this fold can be traced for approximately 2 km along the cliff faces and is particularly obvious in the Hubel region. As many cliff faces and valleys in this region are not true profile sections the shape of many folds, including the Hubel fold (Fig. 6B), tend to be accentuated. It is also difficult to obtain a good idea of the stratigraphic relationships as the units dip gently into the cliff without a good profile being exposed. One of the best sections the Trift Valley is limited in the amount of stratigraphic information it can supply because it parallels the general trend of the fold axes.

### *Trift Valley section*

The area for the best variation of rock types is found in the vicinity of the Trift Valley. The contact of the ophiolite sequence is well-exposed in the Trift Valley and to the north (Fig. 5). The ophiolites here are generally light green to yellow coloured rocks varying from massive to layered (5–15 cm wide) units composed of albite, zoisite and finely deformed chlorite, interbedded with these are fine folded chlorite and sulphide rich layers (BEARTH 1967*a*).

Above the ophiolites is a 3 to 6 m brown-grey Bündnerschiefer, that further to the north is found as occasional outcrops between scree cover. Near the Trift Valley bridge it also contains a dolomitic unit which is highly boundinaged with alternating thick (30 cm) and thin (5 mm) layers and  $F_2$  folds which plunge approximately  $10^\circ$  to  $060$ . The contact with the overlying quartz-phengite schists is very irregular with an angle between the  $S_2$  foliation in the schists and Bündnerschiefer (Fig. 7A) of up to  $30^\circ$ . This observation has also been recorded in other places along strike.

Within the lower section of the quartz-phengite schists two prominent and mapable subhorizontal zones of *rauhwacke* occur as yellow and grey calcareous rocks, which when weathered gives a highly characteristic “honey-combed” appearance. They vary in width from 5 to 80 cm and truncate the foliation in the quartz-phengite schist (Fig. 7B). In outcrop they appear to be monomict *rauhwacke* (LEINE 1968) although occasional portions of polymict material occur, especially where irregular fragments of quartz-mica schist are incorporated. These *rauhwackes* are highly variable in thickness, discontinuous in outcrop and can be mapped northwards from the Trift Valley section as seen in Figure 6A. Very few other occurrences of *rauhwacke* have been recognized except in the vicinity of Hubel fold closure, where they occur as 5 to 20 cm horizons.

The strongly foliated quartz-phengite schists which dominate the Trift Valley are characterized by the presence of small white lenticular quartz bodies that vary



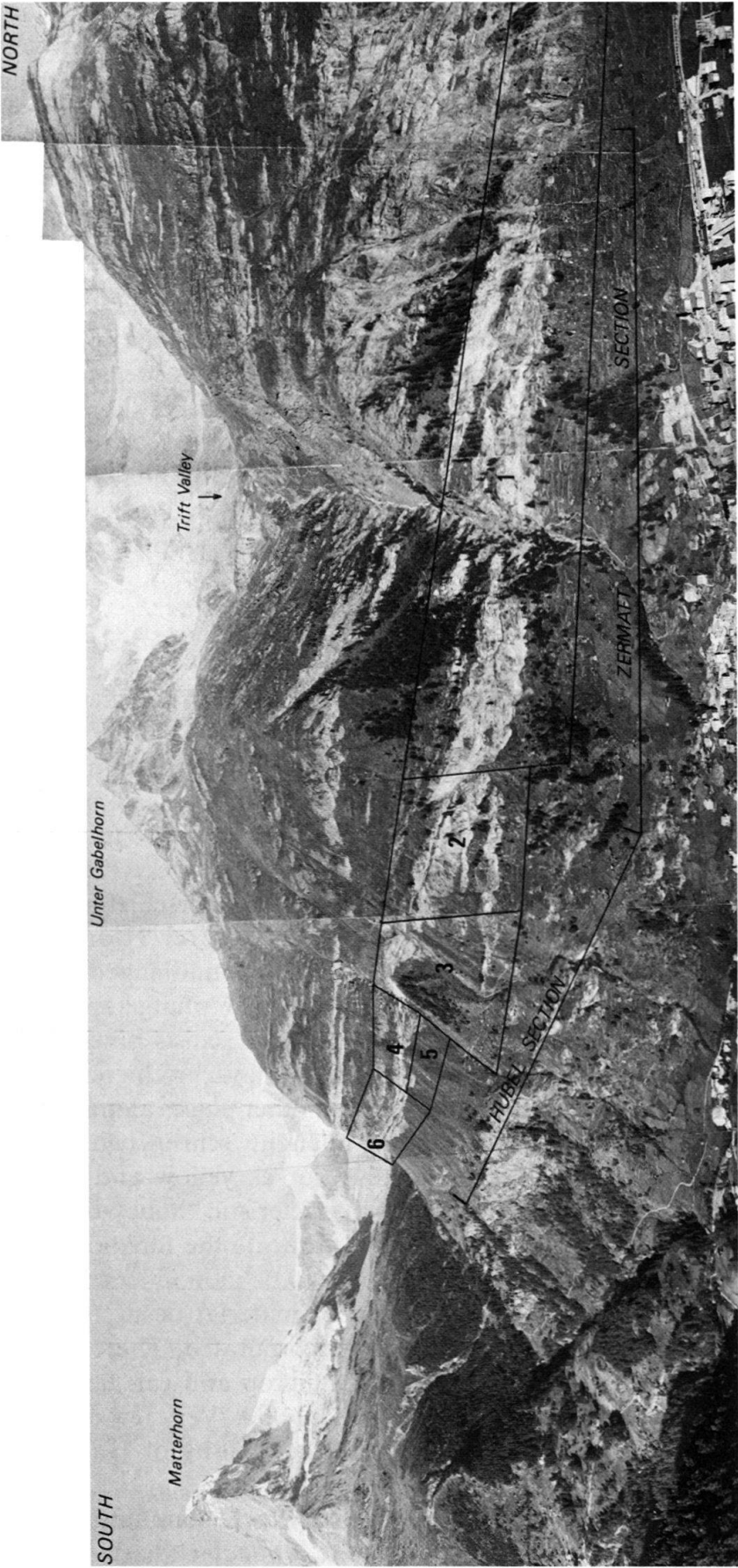


Fig. 4. View of area studied indicating location of Zermatt and Hubel sections (Fig. 6) and structural subareas 1-6.

from 30 cm to a few millimetres, but average between 6 and 3 cm in length. The upper of the two quartz-phengite schists has a higher proportion of calcite, and is separated from the lower unit by a prominent flaggy quartzite unit (Tafelquarzit). The quartzite horizon in these mica schists can be mapped north and south from the Trift Valley in the cliff above Zermatt (Fig. 6) as a unit that is periodically displaced by a series of steep dipping faults.

Between the base of the Bündnerschiefer and the top of the quartz-phengite schists are two conformable quartzite units, separated from one another by a fine recrystallized and laminated 2 m thick calcite-dolomite marble unit that contains few folds. There is extensive boudinage within the quartzites and marbles; the upper quartzite unit varies from 1 cm to 1 m and the lower quartzite attains a thickness of 4 m. At the base of the lower quartzite is another very thin 10 to 60 cm calcite-dolomite marble that is very strongly folded and rests upon the underlying quartz-phengite schists.

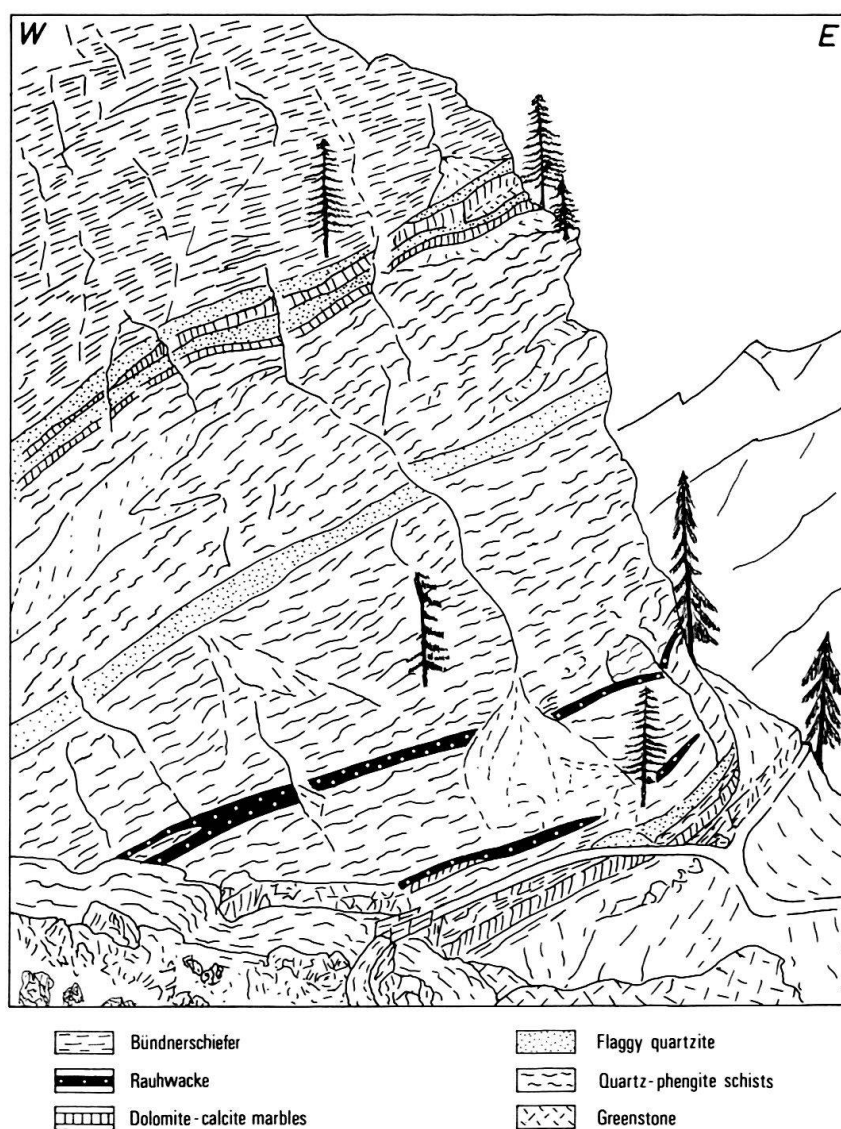


Fig. 5. The section at entrance to Trift Valley west of Zermatt, as viewed from the south (modified after GÜLLER 1947). This section lies almost parallel to the trend of the  $F_2$  fold axes.

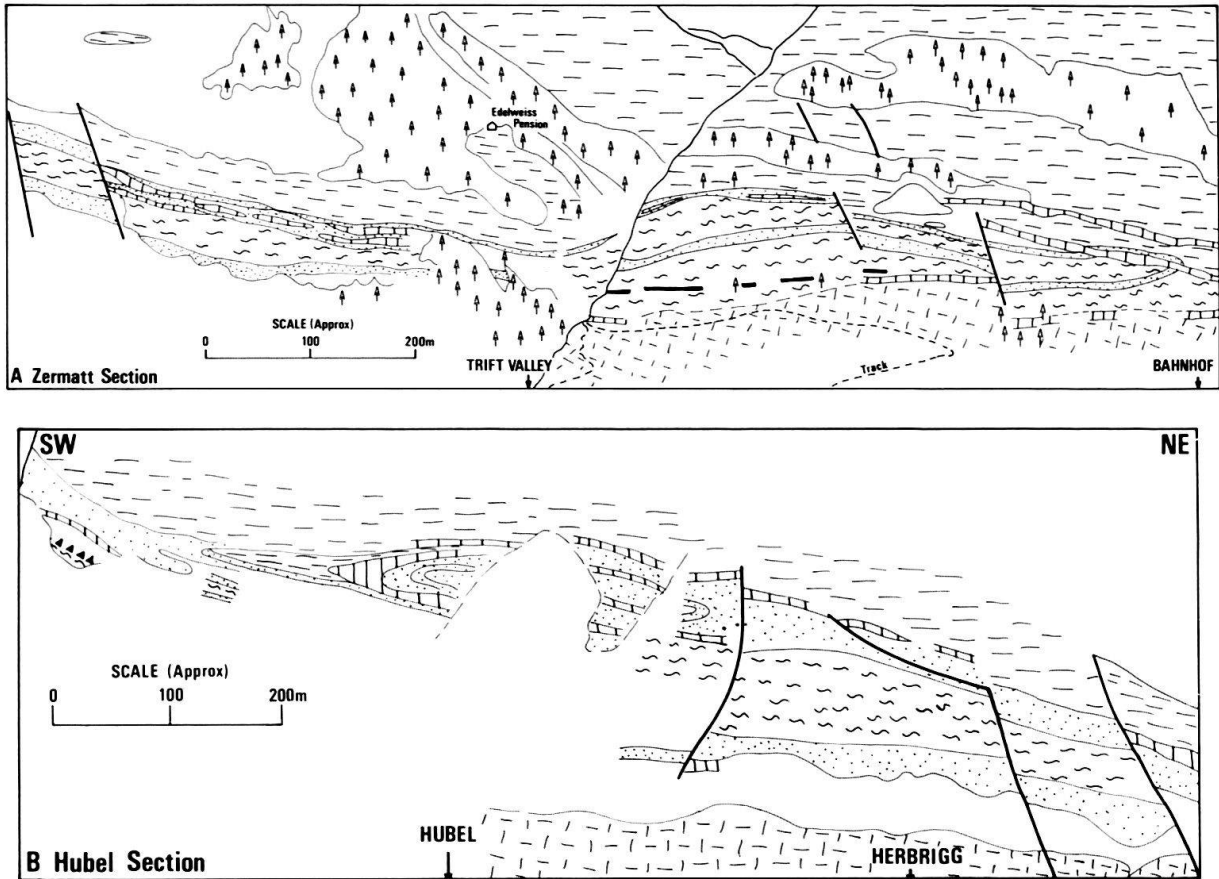


Fig. 6. Sketches of portions of the cliff sections that illustrate the lithological variation at the base of the Theodul-Rothorn Zone. The symbols used for depicting rock types are the same as for Figure 4. The southern end of section A (Zermatt section) overlaps with the northern end of section B (Hubel section). For further explanations see text.

The overlying Bündnerschiefer is a monotonous sequence of strongly foliated calcite-phengite schists containing irregular lenses of calcite that either parallel the foliation or occur as “en échelon” vein structures. Occasional garnet-rich layers are observed, with the mica foliation anastomosing around the garnets. The micas in the Bündnerschiefer are generally curved and give the foliation surfaces a “fish scale” appearance. Folds in the Bündnerschiefer are best exposed on weathered surfaces where the carbonate-rich layers are weathered out; examples of  $F_1$  and  $F_2$  folds can be found in the Trift river section and some 10 m below, and to the south of the Edelweiss Pension good examples of  $F_2$  structures can be observed. 40 m below the Edelweiss Pension there is a prominent zone of deformation, it is characterized by numerous crenulations with irregular axial plane orientations and a large amount of vein calcite. Elsewhere in the Bündnerschiefer are numerous small steep-dipping faults, the surfaces of which are covered with fibrous calcite.

#### *Zermatt section*

The sequence observed in the Trift Valley continues north-east (Fig. 6A), the lower portion containing the quartz-phengite schists, rauhwacke and the ophiolite





Fig. 7A. The angular relationship between foliated quartz-phengite schists (upper unit) and a finely foliated carbonate unit at 623.32/96.75.

Fig. 7B. The irregular contact between a narrow rauchwacke unit and the adjacent quartz-phengite schists at 623.45/96.80. A variably spaced subhorizontal crenulation cleavage is present in the quartz-phengite schists and small  $S_3$  faults transect both the schists and rauchwacke.

boundary, the upper section of quartzite, quartz-phengite schists and Bündnerschiefer is very well-exposed as in the Trift Valley. The rauchwacke cannot be traced continuously along the cliff face and appears as very irregular, discontinuous lenses that are locally folded and faulted. There is no sign of the rauchwacke after a prominent normal fault at the northern end of the cliff section, here the ophiolite contact has been downthrown to the north. Adjacent to this normal fault are numerous post- $F_2$  deformation features, namely crenulation cleavage and small steeply dipping faults.

To the north of this fault the sediments dip gently into the cliff face at approximately  $20^\circ$ , however, they become more steep and truncated adjacent to a 1 to 3 m thick strongly folded calcite-dolomite marble unit (Fig. 6A). This marble corresponds to the marble observed at the base of the Bündnerschiefer in the Trift Valley; it differs from the latter in that there is a lack of associated quartzite and the two marble units have converged to form one unit. The marble contacts are quite complex, along its base there is some rauchwacke and a marked discontinuity in strike. The upper contact of the calcite-dolomite marble unit contains discontinuous lenses of quartzite, above this there is a zone of Bündnerschiefer approximately 12 m wide that is highly brecciated, crenulated and possess numerous extension fractures that are generally oriented normal to the contact and infilled with calcite or siderite. The angular relationship between the contorted Bündnerschiefer and the contact with the calcite-dolomite marble is markedly discordant. Similarly the upper contact of this 13 m zone of contorted Bündnerschiefer is discordant to a relatively undisturbed 4 m horizon of dolomite within the Bündnerschiefer sequence.

Correlating the northern Zermatt and Trift Valley sections with the units observed on the south side of the Zermatt section (Fig. 6A) suggests that the Trift Valley contains a small fault with the southern block being displaced downwards relative to the northern. The upper part of the sequence observed in the Trift Valley continues south until the first major steep-dipping fault. The lower portion, containing the quartz-mica schists and *rauhwacke*, is covered by scree. The upper, finely laminated calcite-dolomite marbles and quartzites are very lenticular and in places boudinaged, highly folded, and extremely variable in thickness (Fig. 15) varying from 50 cm to 3 m. This section is downthrown by the two prominent normal faults that occur at the southern end of cliff of the Zermatt section with the ophiolite contact being upthrown on the south.

### *Hubel section*

The Hubel section contains similar units to the other sections. However, the Hubel fold closes to the south-west and into the cliff face consequently the numerous minor folds developed in the hinge region and projected along the southern portion of the cliff face results in a complex repetition of units, often separated by small subhorizontal faults. These complications have been simplified in Figure 6B.

In the southern end of the section the upper boundary between the Bündnerschiefer and a thick laminated quartzite sequence is a well-defined, low-dipping, conformable contact that continues through to the Hubel fold. Within the quartzites is a thin layer of finely foliated calcite marble. Separating the quartzites from a lower quartz-phengite schist sequence is an 80 cm breccia zone; devoid of folding and parallels the foliation within the adjacent quartzites and schists. The breccia contains appreciable quantities of lenticular quartz set in an anastomosing phengite matrix between which are highly fractured and broken quartzes.

Within the Hubel fold closure are folded quartzites and calcite marbles, a penetrative foliation is often developed in the marbles, especially in the more micaceous portions, in the quartzites there is practically no foliation, only a strong lineation. Between the Bündnerschiefer and the Hubel fold is a distinct quartzite and two calcite-dolomite marble horizons similar to those observed in the Trift and Zermatt sections; however, these units could not be traced further south. It should be noted that nowhere was the Bündnerschiefer / marble-quartzite contact observed to be folded by the Hubel fold. Instead there seems to be a marked discordance in dip and strike between units in the fold and this contact, although this could not be established with certainty because of paucity of outcrop. The northern part of the upper limb contains a *rauhwacke* (30 cm to 1 m thick), it disappears northward under scree cover.

On the northern side of this prominent scree cover is a thick sequence of finely laminated quartzites at the base of which is a highly folded marble unit; this is disrupted by a fault. On the northern side of the fault the sequence continues through to where it joins the Zermatt section, although disrupted by two other faults it is essentially identical to that section. The base contains calcareous schists and marbles and rests on ophiolite, the contact parallels the foliation of the overlying sequence and dips north-west at approximately 30°.

### Fold succession and geometry

#### *Pre- $F_2$ deformation*

In a summary of previous structural work in the Pennine nappes AYRTON & RAMSAY (1974) suggest that two major folding phases occur prior to the superposition of the crenulation cleavage event referred to as  $F_2$  in this paper. From mapping this small area in the Theodul-Rothorn Zone no evidence for a deformation event earlier than what is referred to here as  $F_1$  could be established. Although it is recognized that some of the major nappe units and other zones described by BEARTH (1953, 1964) have probably been established prior or during the event described here as  $F_1$ . Large-scale fold structures resulting from the  $F_1$  event have not been recognized. Thin discontinuous layers within the Bündnerschiefer contain isolated refolded intrafolial folds (Fig. 8), the axial planes of the earliest folds parallel a mica schistosity and are folded by  $F_2$  folds. Comparable structures have been observed in the thin marble units, however in this case, the fine mylonite layering is believed to be of  $F_2$  in origin. Therefore the earliest recognized folds in the marbles may be  $F_2$  and not  $F_1$ .

Much of the evidence for  $F_1$  structures has been obliterated by transposition and by later events. It is often difficult to establish whether they originated as limb areas on  $F_1$  folds in which part of the fold was tectonically removed or whether the folds are a primary feature. The most convincing evidence that the lenticular  $S$  and  $S_1$  schistositities are associated with  $F_1$  structures is that they are folded by the ubiquitous  $F_2$  folds and overprinted by the associated schistosity, particularly in hinge regions.

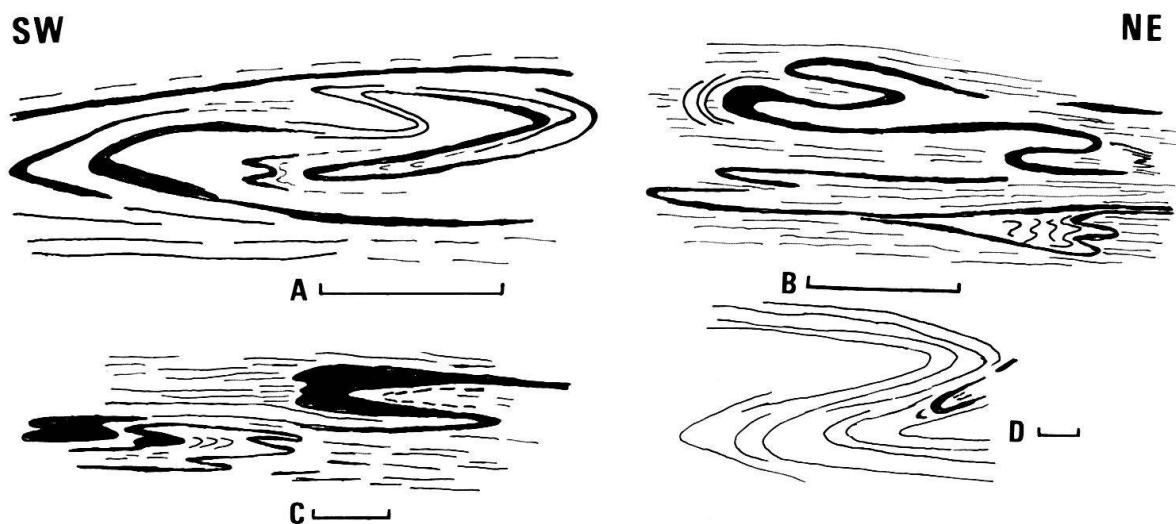


Fig. 8. Profile sketches of features associated with the earliest recognizable fold structures. The sketches are viewed looking west and the bar scale in each sketch equals 10 cm.

- A = Rootless isoclinal  $F_1$  structure folded by  $F_2$  and outlined by marble layers in Bündnerschiefer.
- B = Folded marble layers in Bündnerschiefer containing a fine mica layering that is crenulated in the hinges, elsewhere it parallels the general foliation (folds A and B are from 623.25/96.86).
- C =  $F_1$  fold in quartzite-phengite schist involved in  $F_2$  folding with crenulation cleavage ( $S_2$ ) parallel to  $F_1$  axial planes (at 622.68/96.155).
- D =  $F_2$  structure folding fine Bündnerschiefer layering, within which is a small  $F_1$  fold hinge defined by a marble layer and a crenulated mica-rich area (at 623.22/96.87).

Over most of the area the schistosity dips gently to the north-west, except where it is folded into a steep attitude in the hinge zone of minor folds. As for instance in subarea 4 (Fig. 17) where both  $S$  and  $S_1$  are distributed in a girdle pattern about the  $F_2$  fold axes.  $F_1$  fold axes when observed are approximately coaxial with the  $F_2$  structures.

### *$F_2$ deformation*

In the quartzites and quartz-phengite schists the  $F_2$  minor folds are generally tight to isoclinal structures, with thickened, rounded hinges, attenuated limbs and axial planes parallel the schistosity  $S_2$  (Fig. 9). A consistent regional vergence pattern could be established from the  $F_2$  minor folds even though they are absent over wide areas. The folds verge to the north and have asymmetric, down-plunge Z-shaped profiles which are consistent with the lower limb of the Mischabel backfold.

Asymmetric and symmetric  $F_2$  folds varying from close to isoclinal are present in most of the carbonate units. In the Bündnerschiefer they are characterized by tight long-limbed folds (Fig. 10A and C), some have extremely attenuated hinge zones (Fig. 10F). Similar structures have been recognized in the finely foliated marbles (Fig. 10D). The foliation in the marbles generally parallels the  $S_2$  foliation in the adjacent schists, however misoriented lenses of quartz-mica schist containing  $F_2$  folds and an  $S_2$  foliation may be partly or completely enclosed by finely foliated marble layers. The folding of the marble foliation about such structures is particularly common at the ends of quartz lenses where two marble layers converge and the folds observed vary from open flexures to isoclinal (Fig. 10I). Local thrusting parallel to the axial planes or long limbs of the tight folds is particularly common in these units suggesting that the strain distribution is very inhomogeneous (Fig. 10H).

Isolated refolded intrafolial folds such as shown in Figures 10J and 11 are also observed in the marbles, they generally have plunges and vergences identical to the  $F_2$  structures observed in the adjacent quartz-mica schists. The axial plane structure to the last folding phase is a fine carbonate layering, defined by a poor calcite grain elongation and is similar to the folded foliation. The layering folded by the tight  $F_2$  folds can also occur as a more-or-less penetrative foliation axial plane to isoclinal  $F_2$  fold closures lying within a strong metamorphic foliation. Therefore on the basis of the axial plane structure these folds cannot easily be distinguished from the  $F_2$  structures.

It is believed that these marble layers are zones of very high shear strains in comparison to other lithologies and may represent calcite mylonite zones (see also microstructural observations). The refolded intrafolial folds recognized within these zones of high shear strain may have been initiated as  $F_2$  structures which become progressively flattened and closer to isoclinal during the formation of a fine-grained calcite foliation. So that at high shear strains the planar mylonite foliation developed is a product of the total strain and occurs approximately normal to the direction of maximum finite shortening (i.e. approximately parallel to the  $XY$  plane of the total strain ellipsoid). Then as a result of a relative change in the displacement direction with respect to the trend of the shear zone due to: (1) ductility contrasts between the calcite-calcite and calcite-dolomite layers, (2) an inhomogeneity of



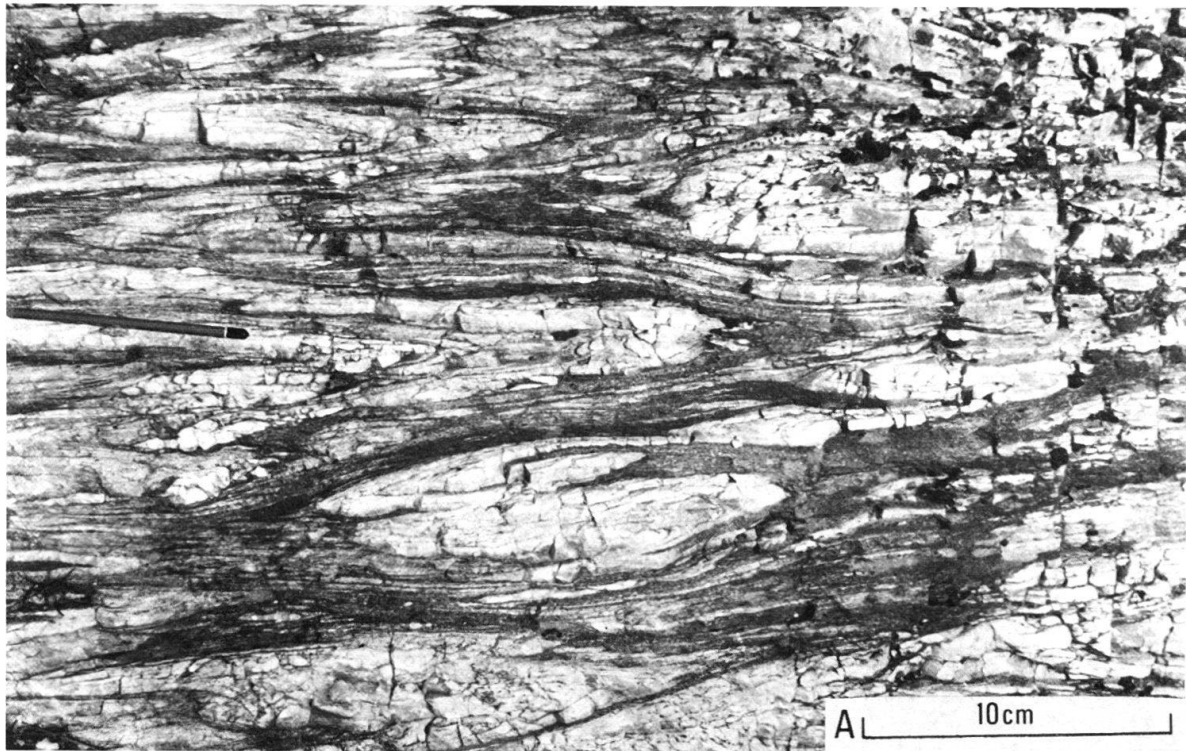


Fig. 9A.  $F_2$  fold profiles in an interlayered quartzite and quartz-phengite schist sequence at 622.66/96.136.

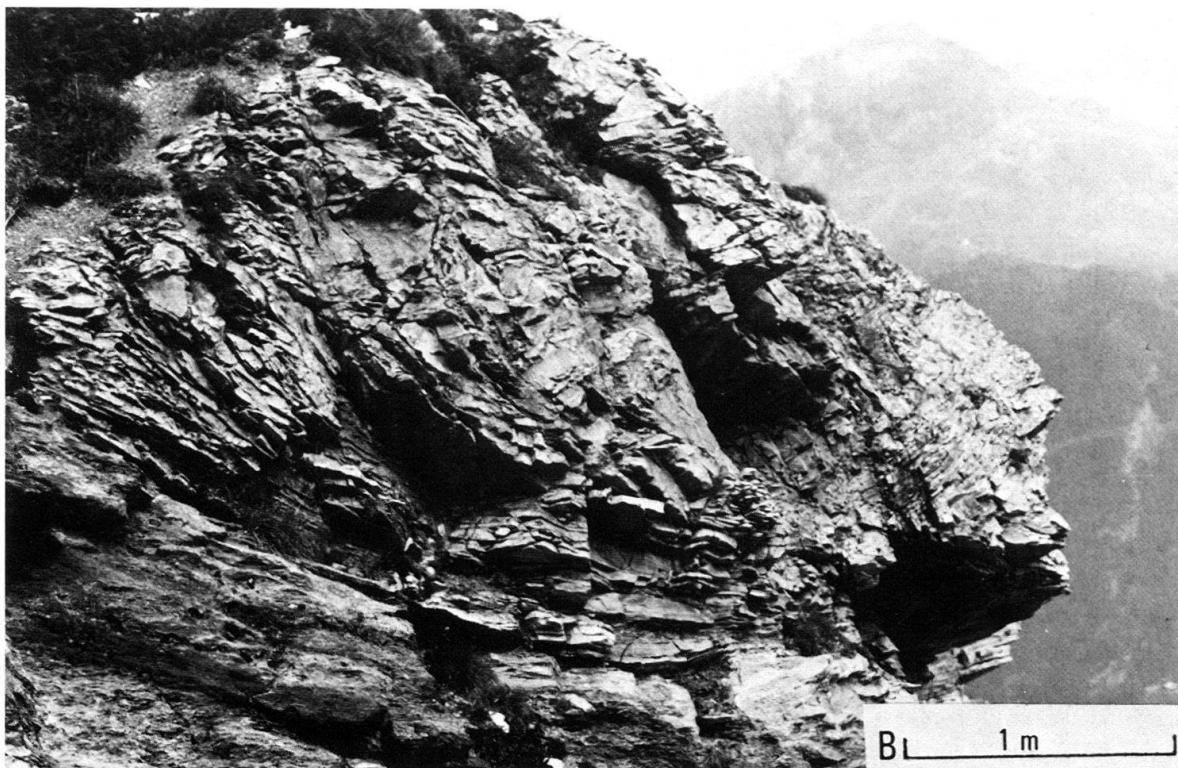


Fig. 9B. Isolated  $F_2$  fold hinge observed in cliff face at 621.91/95.55. The hinge is composed of thin quartzite layers and is enclosed by finely foliated Bündnerschiefer containing small lenses of marble, but devoid of fold closures.

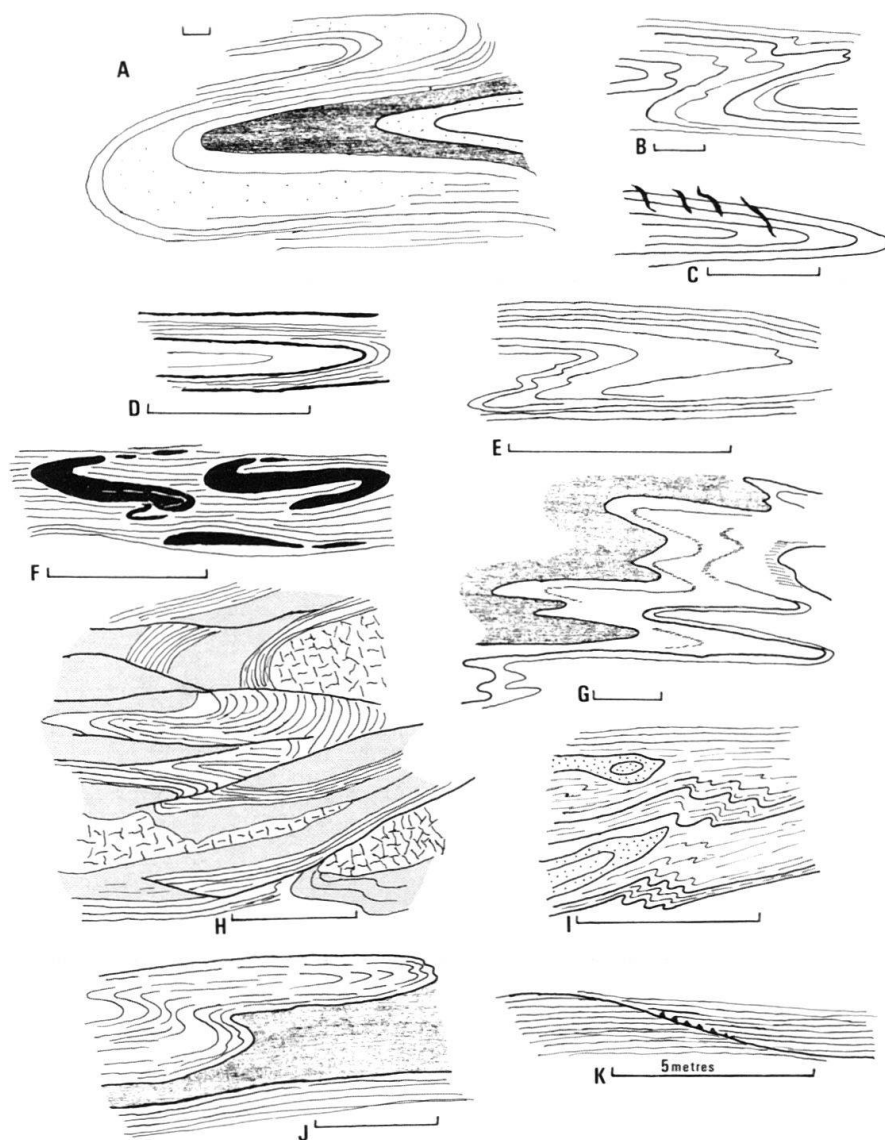


Fig. 10. Selected sketches of deformation features associated with the  $F_2$  recumbent folding and post- $F_2$  shear zones. The sketches are viewed looking west and the bar scale is 20 cm in A-J.

A = Shape of  $F_2$  folds in marbles and Bündnerschiefer at 622.44/95.81.

B =  $F_2$  folds in mica-rich Bündnerschiefer at 623.10/96.67.

C = Isoclinal  $F_2$  fold in Bündnerschiefer at 623.25/96.87. Superimposed on the upper limb is an "en échelon" calcite veining associated with shear zones that predate the  $F_3$  deformation features.

D and E = Intrafolial  $F_2$  folds in marble unit at 623.28/96.73 and 622.56/96.01.

F = Hinges of  $F_2$  folds in marble within Bündnerschiefer at 622.52/95.94. Individual limbs are often highly boudinaged and the direction of necking and elongation parallel the  $F_2$  fold axes.

G =  $F_2$  folds in quartzites and quartz-phengite schists from 622.69/96.14.

H = Small faults associated with  $F_2$  folds in the calcite-dolomite marbles. Adjacent to these faults are sometimes zones of spary calcite. At 623.74/97.15.

I = Oblique section through  $F_2$  folds in quartzite and a crenulated calcite-white mica schist immediately above a mylonitic calcite marble. At 623.10/96.50.

J = Folded  $F_2$  fold in marble interbedded with micaceous marble at 622.69/96.12. The axial plane structure of the folded marble is a grain elongation and is similar to the general marble layering. In the mica-rich area it is a well-defined crenulation cleavage.

K = Subhorizontal thrust in quartzite layers from an area of  $F_2$  folding at 622.38/95.75. Part of this thrust parallels bedding. Where it truncates bedding, units are thinned and brecciated.

strain or (3) the development of an internal buckling instability (COBBOLD et al. 1971), a new set of folds are developed. Such a mechanism has been proposed by CARRERAS et al. (1977) for developing folds in a quartz mylonite. In this way a range of shapes and orientations of folds are developed that fold the earlier fabric elements. This suggests that the tectonic layering produced by the  $F_2$  deformation not only continued to develop during the refolding deformation, but that the  $F_2$  folds were also generated at different stages in this process as a continuation of the  $F_2$ . What appears to be two folding phases may simply be an expression of change in the direction of strain within the narrow marble units; which are in fact zones of inhomogeneous deformation or shear zones.

Also exhibited in the marbles are different stages of well-displayed boudinage and pinch and swell structures that are often associated with  $F_2$  folds. Hinge zones become isolated and limbs may show undulations with pinch and swell structures and boudins. Individual boudins generally have two dimensional lenticular shapes. Paralleling the limbs of many  $F_2$  structures are small faults and thrusts; displacements of 10 cm to 30 m have been recognized. In many cases it is impossible to measure displacements as faults terminate and parallel foliation planes as in Figure 10K.

### *Lineations*

Lineations are chiefly the intersection of the bedding or  $S_1$  with the axial plane cleavages of  $F_2$  folds, and are especially marked in the strongly folded section in the Hubel area. No mineral lineation was observed associated with the isolated  $F_1$  folds. In the quartzites the lineation develops where the  $F_2$  crenulation cleavage cuts the earlier bedding ( $S$ ) and schistosity ( $S_1$ ) and divides the rock into a series of mullions (Fig. 12A), some having rhomboidal shaped cross sections. These mullions lie parallel to the hinge of  $F_2$  minor folds. In the marbles the lineation appears as thin dark and slightly irregular traces across the schistosity and again is parallel to the  $F_2$  fold hinges.

The lineation  $L_q$  lying within the  $S_2$  schistosity surfaces is often parallel to the hinges of  $F_2$  minor folds.  $L_q$  is a form of rodding occurring where the interface between layers of quartz and micaceous quartzite have been deformed into small lobe and cusp structures (RAMSAY 1967). The lobes stand out as parallel rod-like features on exposed surfaces in the schist. They are uncommon features and are found mainly in subareas 1 and 2 where the trend of  $L_q$  lineation is parallel to the minor fold hinge lines (Fig. 12A). In some cases the quartz rods appear to be very thin boudins of vein quartz lying within the  $S_2$  foliation. In portions of the quartz-phengite schists they are so numerous that the rock appears to be a conglomerate (Fig. 11B) and have characteristics similar to the pseudo-conglomerates described by RAMSAY (1956).

### *Shape characteristics of $F_2$ folds*

A series of fold profiles were studied (Fig. 13) in order to describe and interpret representative fold geometries. Thickness variation using the dip isogon technique (ELLIOTT 1968, RAMSAY 1967, HUDDLESTON 1973a) were plotted as orthogonal



thickness versus dip,  $t'_a/a$ . In Figure 13 it can be seen that most hinge zone regions are in either class 1B or tending towards 1C and in some cases attain the geometry of similar (class 2) folds. Some folded layers are more complex and show inflections. This can be attributed to either irregularities in the initial layer thickness (HUD-

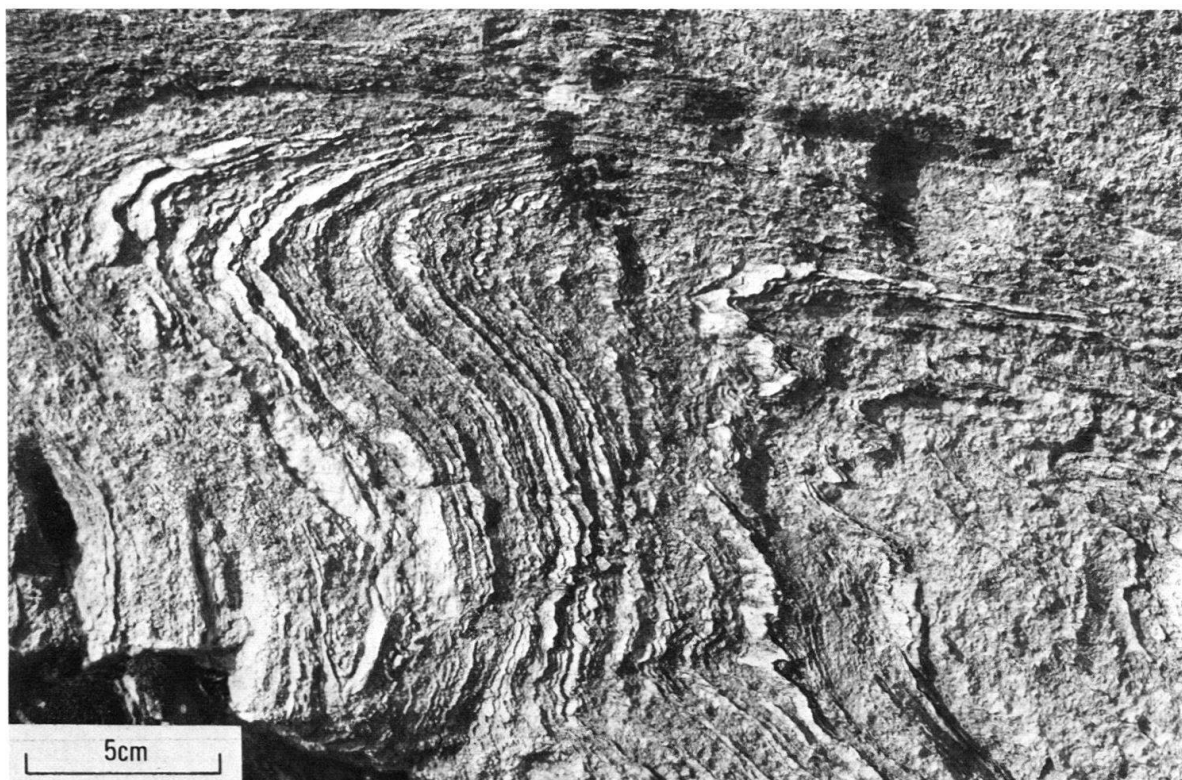


Fig. 11. Refolded isoclinal fold in marble unit at 622.94/96.34.

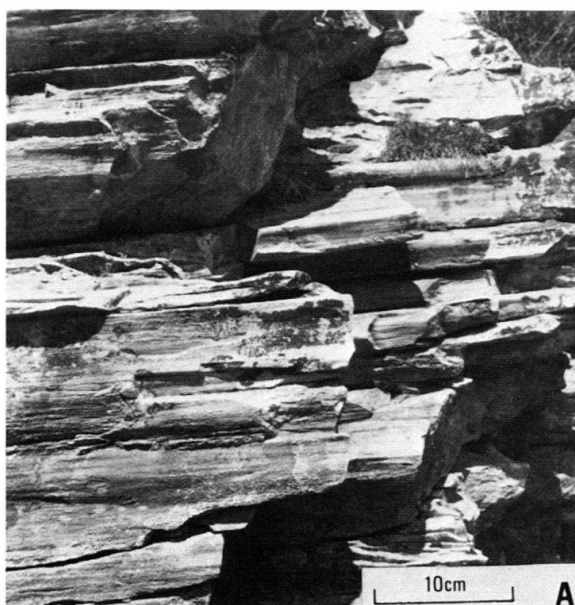


Fig. 12A. Lineation development in the quartzites associated with the Hubel fold closure.

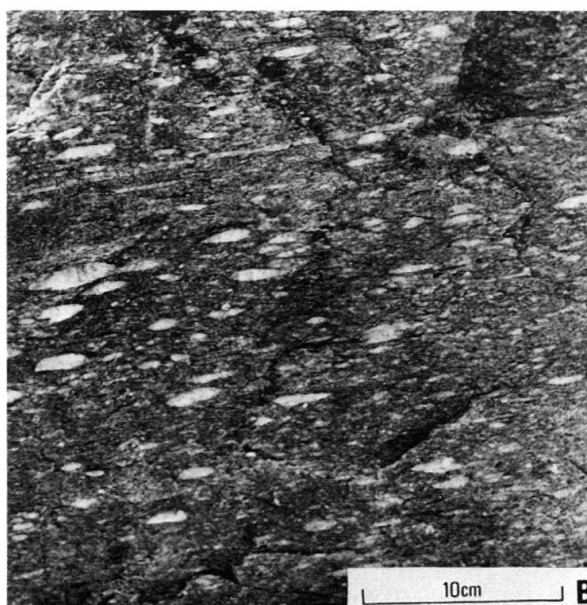


Fig. 12B. Development of pseudo-conglomerate in quartz-phengite schists at 623.01/96.34.

DLESTON 1973*a* and *b*) or a compounding of different fold styles (RAMSAY 1967, p. 371). The variation may also arise locally at the site of parasitic fold hinges; as most of these examples are parasitic fold hinges from within the Mischabel back-fold.

Fold layers that approximate one particular class over their entire quarter wavelength are those of the class 1B, and are observed both in the pure quartzites and some pure calcite marble layers. Class 1C folds are common in the quartzites with minor intercalations of mica schist and tend to have the most irregular  $t'_a/a$  plots (Fig. 13A). This is especially noticable where the thickness of the competent layer is less than or equal to the thickness of the incompetent layer.

The  $t'_a/a$  plots give an idea of the apparent strain ratio  $\sqrt{\lambda_2/\lambda_1}$  if the folds are flattened parallel folds (RAMSAY 1967, Fig. 7-79) or where buckling and flattening proceed simultaneously as in the case of low viscosity contrasts between adjacent layers (HUDDLESTON 1973*a*, HUDDLESTON & STEPHENSON 1973). In the case of folds (*A* and *C* in Fig. 13) where there were high viscosity contrasts between the quartz-rich versus mica-rich layers the curve of RAMSAY (1967) was used and values show a wide range from 0.1 to 0.8 to indicating that any single fold underwent varying amounts of flattening.

From the final fold geometry it is difficult to evaluate a simple mechanism or a combination of mechanisms for the folds in Figures 10 and 13 as it must assume something about the nature of the layers prior to the  $F_2$  deformation, especially their continuity in thickness and shape. Specifying the fold class does not uniquely specify the fold mechanism, finite strain state nor the deformation path. Also the mechanical operations on a submicroscopic scale during the development of a particular fold class may be very complex. As the  $F_2$  folds in the more competent quartzites generally have a class 1 form it may suggest that their formation may involve some degree of buckling (RAMSAY 1967, p. 372). What may be discerned from the fold shapes in Figures 8-13 is an estimate of the percentage of apparent buckle shortening (NAHA & HALYBURTON 1977) and it appears that the majority of the  $F_2$  folds have undergone a shortening of 60-80%. The large values of shortening and the low values of  $\sqrt{\lambda_2/\lambda_1}$  together with a high length/breadth ratio of quartz grains elongated parallel to  $S_2$ , the presence of lense-shaped mica aggregates (cf. WILSON 1978), boudins of vein quartz that give rise to the  $L_q$  lineation all indicate that although the  $F_2$  folds may have been initiated by buckling they were modified by extreme flattening normal to their axial planes. This conclusion is further substantiated by the presence of post- $F_2$  shear zones. Similarly the observation that most folds are class 1C or tending to class 2, the complete absence of layers which are class 1B over their entire length, and the fact that most layers are class 1A in the hinge and become class 1C in the limbs are consistent with an element of homogeneous (RAMSAY 1967, p. 434) or simultaneous flattening and buckling (HUDDLESTON 1973*a*).

Alternatively it is possible to account for the properties of these folds in terms of a model involving simple shear (RAMSAY 1967, p. 421-437). HOBBS (1971) has pointed out that the larger the flattening strain the smaller the amount of simple shear required to produce a given fold shape similarly the smaller the flattening strain the larger the amount of simple shear.

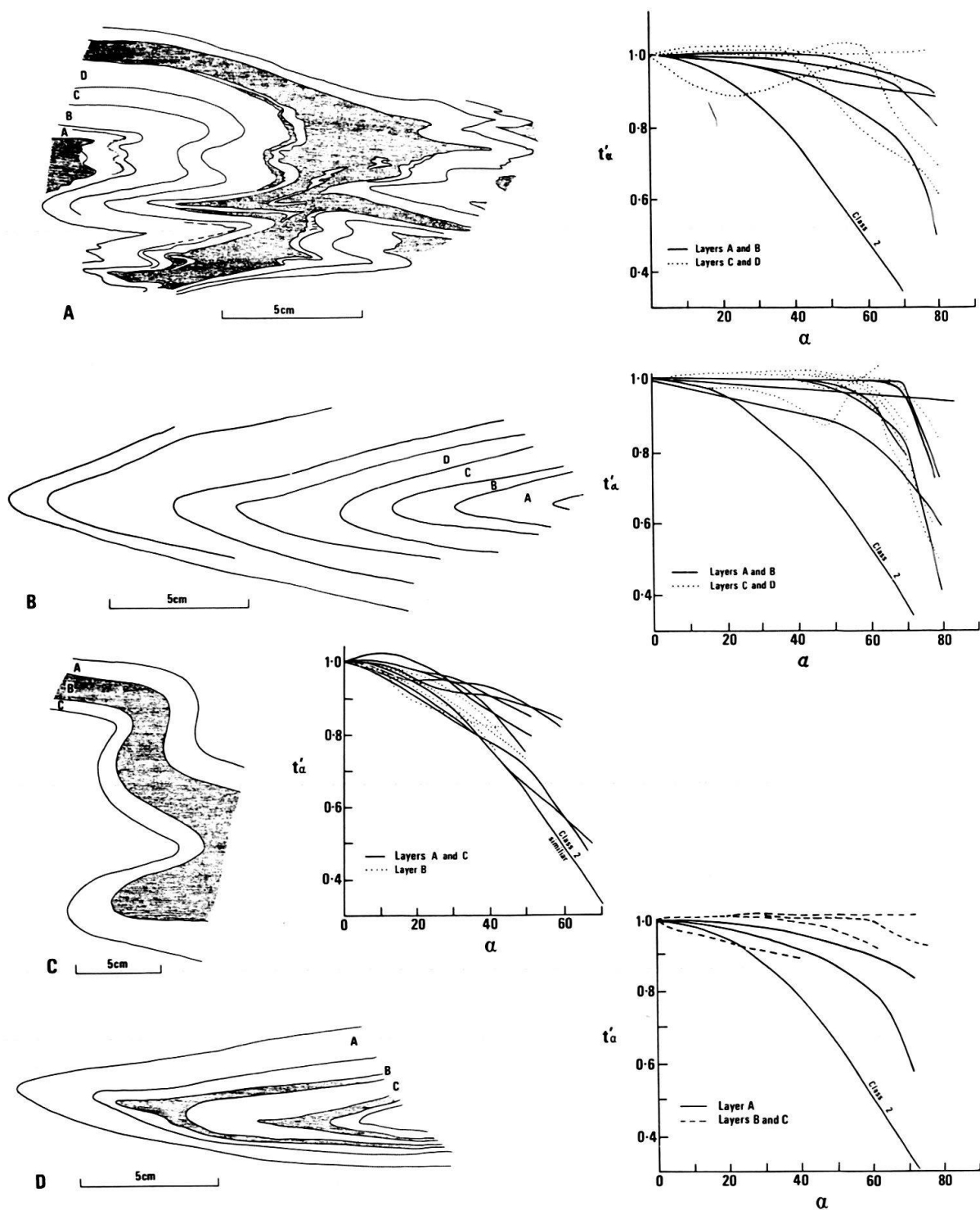


Fig. 13. A series of representative  $F_2$  fold profiles. The hinges are generally thickened and one limb is consistently thinner than the other. The folds are tight and have pointed hinge zones in the micaceous layers with interlimb angles varying between  $40^\circ$  and  $20^\circ$ . The dip isogons are subparallel and convergent in the quartzite layers. The folds are taken from: (A) Quartzite within quartz-phengite schist at 622.644/96.130, a variation in tightness is observed between individual folds; (B) Quartzite from 621.67/96.52; (C) Quartz-phengite schist at 622.35/95.75; (D) Quartzite containing phengite-rich layers from 622.66/96.130.

*Post- $F_2$  shear zones*

Intersecting some  $S_2$  foliation planes at angles varying from 5 to 30°, as a series of subhorizontal surfaces are microscopically visible shear zones (Fig. 14). They are particularly obvious in rocks collected from the lower portion of the Mesozoic sequence and are abundant in the quartzites adjacent to the finely laminated calcite marbles. Recognition of these features in the field is often difficult, however, the presence of irregularly distributed button-shaped mica aggregates (ROPER 1972) in the micaceous schists an asymmetric crenulation with a wide spaced wavelength (2–5 cm) superimposed on the  $S_2$  foliation are usually indicative of their presences. The crenulation cleavage (Fig. 14B) is only very locally developed in highly anisotropic quartz–phengite schists, it parallels and is often associated with the micro-shear zones observed in thin section. In the marbles small (Fig. 10H) subhorizontal thrusts are commonly observed lying subparallel to the margin of the marble units. Such zones have also been recognized in the Bündnerschiefer, together with “en échelon” vein type shear zones (Fig. 10C). In all cases these features are overprinted by the  $F_3$  structures.

In the marbles the shear zones are particularly obvious in association with the development of pinch and swell structures (Fig. 15). The pinch and swell structures are responsible for the thickening and thinning of marble units where they are interbedded with quartz–phengite schists and their development may be a result of buckling instabilities in the marbles and hence reflect a low anisotropy contrast between these and the adjacent schists as well as the orientation to the maximum compression direction. For instance if the maximum compression direction acts at a high angle to the pronounce  $S_2$  foliation then pinch and swell structures similar to those envisaged by COSGROVE (1976, Fig. 6) will develop.

The small thrusts or shear zones associated with the marble pinch and swell structures would then reflect an internal instability. Thereby acting as a means of

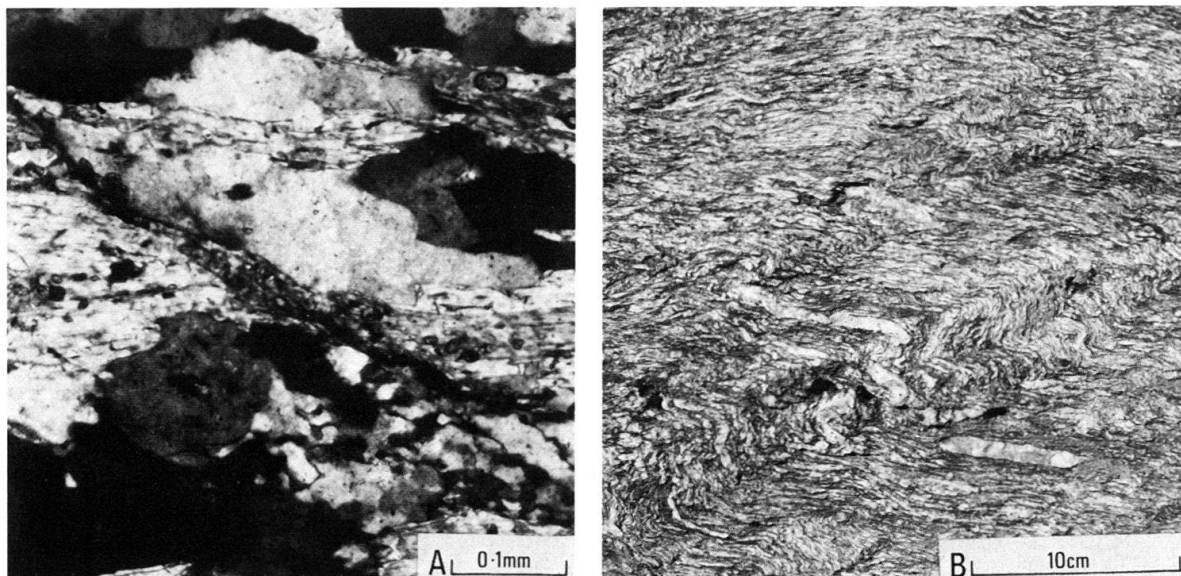


Fig. 14A. Photomicrograph of small shear zone in quartz–phengite schist.

Fig. 14B. Crenulation cleavage folded  $S_2$  foliation in quartz–phengite schist.



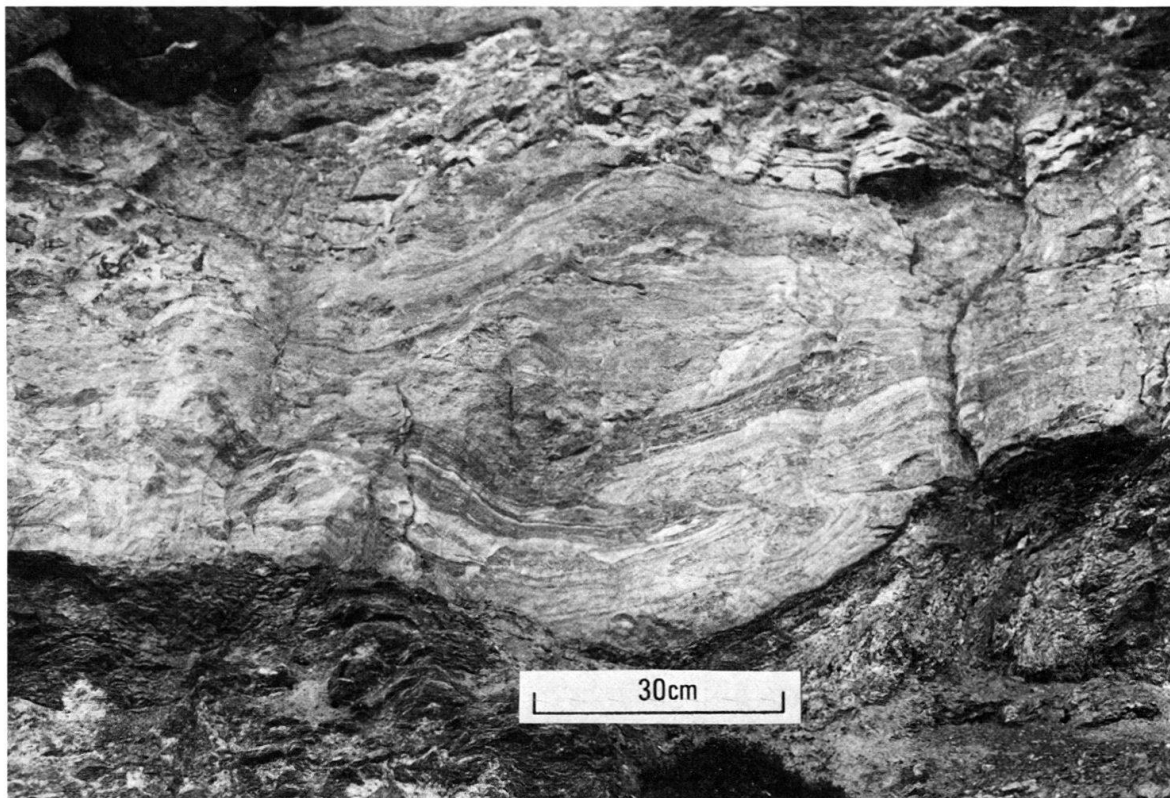


Fig. 15. "Pinch and swell structure" displayed by calcite-dolomite marble at 623.74/97.15.

accommodating the external shape change and hence must be closely related in orientation and origin to the pinch and swells. Similarly the microshear zones and associated crenulation cleavage in the quartzites and quartz-phengite schists may represent a situation of high anisotropy contrast as discussed by COSGROVE (1976). Thus the style of deformation in the shear zones is coupled with the quite different mechanical properties of the individual minerals in the quartz-mica rich layers in comparison to the marble layers.

The reason for including these shear zones within the  $F_2$  deformation event is that most rocks bear some imprint of the shear zone event, and it is often impossible to isolate it from the main  $F_2$  deformation features. This is particularly obvious in the quartz microstructure (C.J.L. Wilson, unpublished data). In part the flattening of the  $F_2$  folds may have occurred during this period of the deformation. The late change in deformation style may be related to the thickening of the tectonic sequence during the formation of the Mischabel backfold. However, unlike the hypothesis presented by RUTLAND (1965) for tectonic overpressures there is no mineralogical evidence to substantiate the present interpretation. In fact the modification of the  $F_2$  deformation features by the shear zones appears to be local accommodation to a change in the physical conditions. This event may not be obvious outside the area described here. It should also be noted that the strain path during this  $F_2$  deformation could be quite complex and may involve simple and pure shear together with the shortening across the Mesozoic sedimentary sequence.

### *F*<sub>3</sub> deformation features

These are a group of structures that overprint all other major deformation features and are collectively called *F*<sub>3</sub>, they include a group of crenulation cleavages, kink folds, faults, chlorite- and quartz-filled gashes and tension gashes that have a near vertical orientation. From field evidence it is clear that the majority of the subvertical *F*<sub>3</sub> structural features are in fact different from the subhorizontal microscopic shear zones associated with the *F*<sub>2</sub> deformation as they consistently overprint the earlier structures.

The *kink folds* are small asymmetric structures (Fig. 16A) the majority of which occur in the quartz–phengite schists, others are found in thinly laminated quartzites. Their steep-dipping axial planes (*S*<sub>3</sub>) strike north-west and the hinge lines of the kink folds (*F*<sub>3</sub>) generally plunge gently north (Fig. 17). Where a kink's axial plane is propagated into a quartzite horizon small often closely spaced faults or joints are observed that maintain the same orientation as the axial plane of the kink.

The *joints* may either be barren joints or infilled with quartz, often with a fibrous appearance, and/or chlorite. The vein filling material appears to be locally derived, as the rocks immediately adjacent or with the vicinity of the joints are depleted of quartz and are often fractured for a distance up to 1–2 cm (Fig. 16B). Barren joints

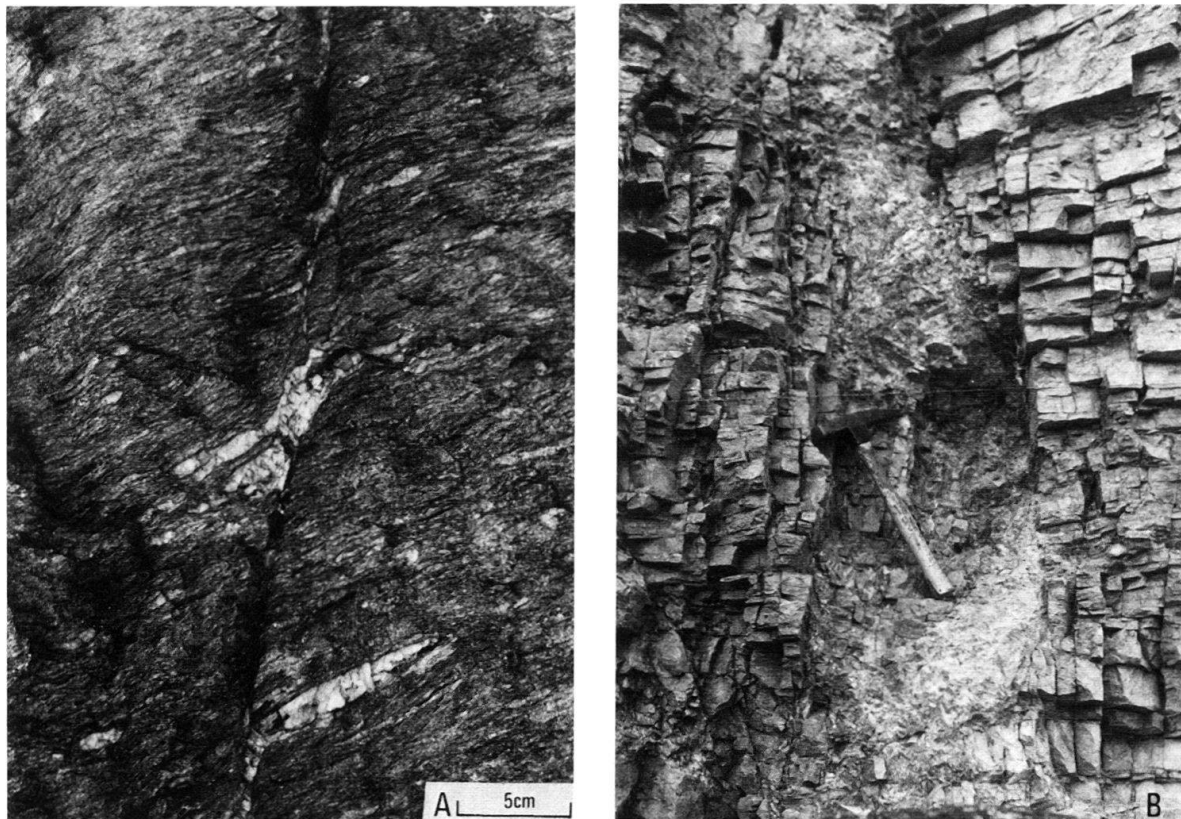


Fig. 16. *F*<sub>3</sub> deformation features. (A) shows the development of kink-like folds and associated displacements in quartz–phengite schists. (B) jointing in more massive quartzites. Length of hammer handle is 30 cm.

are considerably more common than both quartz- and chlorite-filled joints. They intersect all rock types and commonly occur parallel to  $S_3$  orientation.

*Faults* were distinguished in the field by the observable displacements across them, nearly always in a normal sense. Most distinct faults have displacements of less than 5 m, but a few faults with throws greater than 50 m have been observed (see faults in Fig. 5). These larger faults especially in the quartzites often occur as zones up to 2 m in width, the margins of which are strongly jointed with numerous barren joints. The strike and dip of the faults show the same general trend as the barren joints, so there may be a close genetic relationship between these structures.

### *Macroscopic geometry*

The geometry of the foliations, fold axes and lineations for the area at the base of the Unter Gabelhorn is depicted in Figure 17. The area has been subdivided into 6 subareas (Fig. 4) which are characteristic of particular rock types and structures.

All subareas are characterized by strong  $S$  and  $S_1$  pole concentrations confirming the gentle north-west dip, comparable  $S_2$  pole orientations are also observed. Subarea 4, the region of the Hubel fold closure is characterized by a change in attitude with a spread of poles to  $S$  and  $S_1$  in a great circle about a westerly plunging axis.

$F_2$  fold axes show different distributions from one subarea to another. In subareas 1 and 4 there is a tendency to plunge subhorizontally in a westerly direction.  $F_2$  folds in subarea 2 have gentle plunges both to the south-west and north-east in any single outcrop about a common axial plane orientation. Poles to the axial planes in subarea 2 form a partial girdle, which may be explained by rotation between adjacent subvertical fault blocks (cf. Fig. 3). In subareas 3 and 5 there are both northerly and north-westerly subhorizontal plunge directions. Subarea 6 contains very few  $F_2$  folds as the cliff parallels the fold axis direction, and displays limb area geometry.

The marked fold axis orientation differences from one subarea to another can also be seen in individual outcrops, for example parasitic folds on the upper limb of a fold may have a different orientation to those on the lower; between the two limbs are small thrusts. This also appears to apply on a larger scale, however as these thrusts parallel bedding they may not be recognizable.

$L_q$  lineations in subareas 1 and 2 display two prominent elongation directions either west or north. They are almost perpendicular to one another and nearly parallel to many of the folds observed in these subareas.  $S_3$  surfaces are generally subvertical except in subarea 3 where gentle dips are visible and these are related to later faulting. The few measurable  $F_3$  folds have gentle plunges which are governed by the local orientation of the earlier  $S$ ,  $S_1$ , and  $S_2$  schistositities.

### **Conditions of metamorphism and microstructure**

In the sediments of the Theodul-Rothorn Zone there is a notable absence of critical bulk rock compositions and mineral assemblages that preclude making a definitive statement about the range of temperature, pressure and any fluid compo-



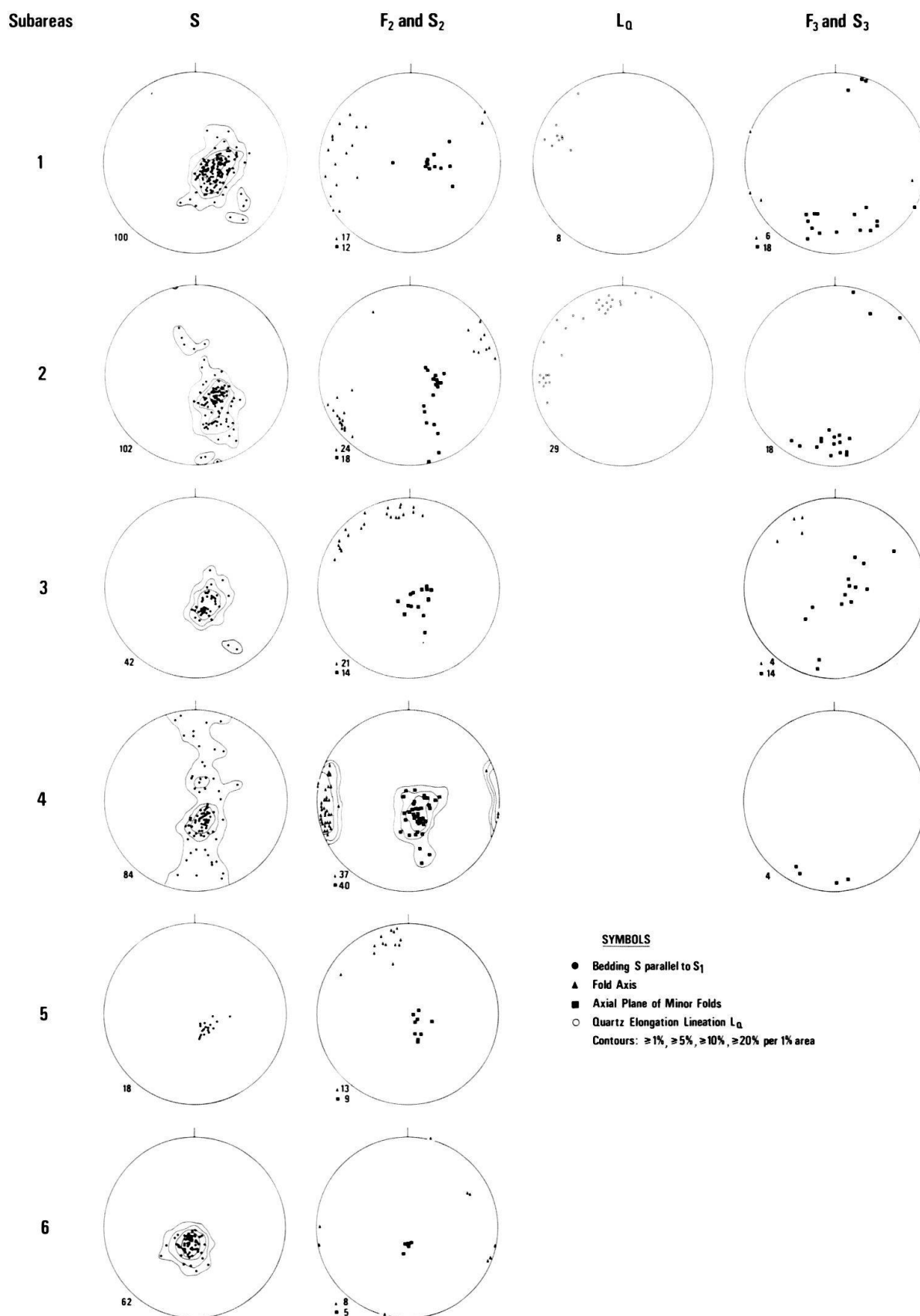


Fig. 17. Representative geometry of fabric elements in the subareas shown in Figure 4.

sition during the deformation of this unit. An idea of the metamorphic conditions may be obtained from the adjacent units, where two main periods of metamorphism may be recognized as summarized in FREY et al. (1974) and COMPAGNONI et al. (1977).

The Zermatt-Saas Zone that underlies the Theodul-Rothorn Zone is a typical ophiolitic suite (BEARTH 1967*a*) that has first undergone a high-pressure facies early Alpine Upper Cretaceous event followed by a lower pressure and higher temperature Greenschist facies metamorphism (upper Eocene-lower Oligocene, Lepontine event). The high-pressure event is responsible for the formation of the eclogites and glaucophane schists (BEARTH 1962, 1967*a*) with assemblages including omphacite, jadeite, garnet, glaucophane, chloritoid, kyanite and various white micas. The low or intermediate pressure Greenschist facies metamorphism has overprinted these assemblages with chlorite, blue-green amphibole, actinolite and in some place later glaucophane (BEARTH 1967, CHADWICK 1974). In the Obere Zermatter Schuppenzone (BEARTH 1964) that overlies the Theodul-Rothorn Zone the assemblages correspond with the Greenschist facies metamorphism. Whereas the overlying Arolla Series (correlative with the Sesia-Lanzo Zone, CARRARO et al. 1970) exhibits the effect of the high-pressure facies metamorphism (DAL PIAZ & NERVO 1971; DAL PIAZ et al. 1977).

Unlike the adjacent zones the Theodul-Rothorn Zone has only experienced the later 38 m.y. (BOCQUET et al. 1974) Greenschist facies metamorphic imprint and does not seem to have suffered the high-pressure / lower temperature conditions of the early Alpine phase. Observations made by the writer revealed that the main mineral nucleation is the result of the Greenschist facies regional metamorphism. Further evidence for this is presented by DAL PIAZ et al. (1972) and also supported by the work of KIENAST (1973) who uses data from the Si-cation content of the phengites. During the present investigation values for the  $b_0$  spacing in the phengite micas from the Theodul-Rothorn Zone were obtained using the method of SASSI (1972). The values scattered between 8.994 and 9.010 Å, and suggest that the micas nucleated during the lower pressure metamorphic event.

The principal metamorphic minerals in the quartzites are quartz, phengite, albite and chlorite; in the calcareous schists are calcite, dolomite, quartz, phengite, epidote, graphite, garnet and a blue-green amphibole. As the Greenschist facies metamorphism is accompanied by the multiple deformation, then the earliest formed metamorphic assemblages are reworked during the subsequent deformation and it is possible to relate the timing of the metamorphism to the various phases of deformation. Microstructural evidence indicates that the nucleation of these minerals in the Theodul-Rothorn Zone is associated with the  $F_1$  deformation event. During the  $F_2$  deformation event no new mineral phases were nucleated instead all the earlier assemblages were deformed, only the carbonate minerals underwent extensive recrystallization or grain growth.

In the quartzites and quartz-mica schists the  $S_1$  microstructure is rarely preserved in the sequence, the quartz grains are highly sutured, with undulose extinction and have a strong dimensional orientation. Individual micas, especially on the limbs of  $F_2$  folds are either lenticular or appear to be boundinaged. Whereas in the hinge region of the same folds the micas appear to have undergone some process of

recovery for they form “polygonal arc” type structures (MISCH 1969), as shown in Figure 18A. Albite and potassic feldspar porphyroblasts in the quartzites appear to have been nucleated and grown with these muscovites but are also deformed showing undulose extinction and the mica foliation is deflected around them. During the  $F_2$  deformation the albite porphyroblasts were sometimes slightly rotated so that the rare inclusion trails lie at a variable angle to the schistosity, and triangular shaped spaces infilled with quartz occur at their ends (pressure shadows).

There are also a large number of calcite-quartz layers that are generally parallel to the major compositional layering and schistosity, although others clearly transgress the very fine schistosity particularly in the schists. All the thicker sheets (from 5 mm to 20 cm) are now boudinaged. The calcite-rich sheets are usually composed of recrystallized grains with occasional cores containing large twinned grains. Whereas the quartz, although commonly recrystallized does show relic portions of the primary crystals. Such relics may be zoned with their  $c$  axes parallel to the vein margins, and are surrounded by a recrystallized margin. These quartz-calcite bodies appear to have developed in association with the  $F_2$  deformation event, as they are generally observed lying parallel to  $F_2$  axial surfaces and are disrupted by the  $F_3$  deformation events.

The calcareous schists have modal compositions that vary greatly and the schistosity is less pronounced than the quartz-phengite schists. The microstructure is dominated by coarse- to medium-grained calcite that is variably deformed, displaying intracrystalline deformation features such as undulose extinction, subgrains, kinks and twinning. Recrystallization occurs only in the highly deformed rocks with new grains being nucleated on grain boundary margins and in kinks and twins (Fig. 18B). Thin dolomite layers (1 mm to 30 cm) are often interlayered with the calcite portion of the rocks and are generally conspicuous by having a finer grain size than the adjacent calcite layers. Occasional layers rich in ferroan calcite (determined using the staining technique of DICKSON 1965) are commonly associated with calcareous schists rich in chlorite. Mica-rich layers and layers containing elongate quartz grains alternate with the calcite and dolomite layers. The micas are conspicuously lense-shaped and boundaries between adjacent calcite and quartz grains are generally embayed. Some mica-rich layers are accompanied by concentrations of hematite, particularly along mica/mica and calcite/mica boundaries. Hematite concentrations appear to be superimposed on the micas and are locally irregular, truncate and/or transgress individual calcite or mica layers. The calcites adjacent to the hematite-rich layers are generally altered to a ferroan calcite. The embayed and lenticular mica microstructures strongly suggest that the boundaries have been modified by water assisted diffusional processes (WILSON 1977). The conspicuous hematite concentrations appear to be superimposed and truncate these earlier microstructures and also appear to originate from a water assisted diffusional or transport process such as “pressure solution”, and could be referred to as a stylolite (BATHURST 1971). It appears that the earlier event is intimately associated with the development of the  $F_2$  microstructure whereas the later solution effect could be  $F_3$  or latter.

The white and cream coloured marbles are dominantly calcite-rich with occasional dolomite layers. They vary from coarsely crystalline rocks with little quartz,

no feldspar and a small percentage of white micas to finer grained types (grain diameters of 0.25 to 0.13 mm), as in the folded marble units observed in the Hubel folds closure. Solution effects between grains are very obvious in these marbles.

The fine grey-white layered marbles close to the Bündnerschiefer boundary and adjacent to the Zermatt-Saas Zone are generally composed of fine recrystallized calcite, within which are larger deformed calcite grains or porphyroclasts (Fig. 18C and D), and deformed white mica. The grey-white colour layering, which represents both grain size and compositional differences, may be deflected around aggregates of porphyroclasts. These marble layers resemble recrystallized calcite mylonites (cf. SCHMID 1975). There is generally little obvious solution effects recognized within the central region of the recrystallized marbles, however their margins may show extensive alteration and in places resemble a *rauhwacke*.

The rock type recognized in the field as a *rauhwacke* is generally a calcite-dolomite breccia, angular fragments of layered dolomite occur in a fine-grained laminated calcite or ferroan calcite-rich matrix. The matrix may also contain solitary quartz grains or quartz aggregates that vary from underformed euhedral crystals exhibiting crystal growth features to highly deformed and elongate grains. Unlike other *rauhwackes* (WARRAK 1974) there appears to be an absence of gypsum or anhydrite. Deformed white micas exhibiting abundant kinking, subgrain formation and having (001) cleavage surfaces stained with hematite are ubiquitous.

In nearly every thin section of *rauhwacke* examined there are variable quantities of iron oxide, with the highest concentrations being observed along grain boundaries. These observations suggest that there have been appreciable solution effects within these rocks. The relative contribution of metamorphic fluids versus meteoric fluids cannot be distinguished and is similar to the problem encountered by WILSON (1977). It is probably significant that the matrix of the *rauhwacke* is always dominated by a fine grain size as this may account for the abundant evidence of fluid transport. As it is now well-established that by decreasing grain size during plastic deformation there is an increase in the rate of deformation with strain softening (ASHBY & VERRALL 1973; KERRICK et al. 1977). This is accompanied by a change of deformation mechanisms from dislocation dominated processes to diffusive or superplastic processes (SCHMID et al. 1977). Hence the zones of *rauhwacke* may in fact be zones of very high strains, extensively altered and modified by the later diffusive processes. A similar explanation for very high strains in narrow quartz mylonite zones has also been suggested by WHITE (1976).

---

*Explanations to Figure 18*

A = Optical micrograph of folded mica-rich area from the specimen illustrated in Figure 13A. Most micas are deformed and parallel the axial surface, however in the hinge (at *a*) and on one limb (at *b*) there is a bimodal mica distribution.

B = Micrograph of typical deformed marble exhibiting kinked calcite, bent white micas and smaller recrystallized calcite grains.

C = General micrograph showing foliation in mylonitic marbles; it is defined by the porphyroblasts and small micas.

D = Detailed micrograph of calcite mylonite showing relic twinned porphyroblasts surrounded by recrystallized calcite grains.



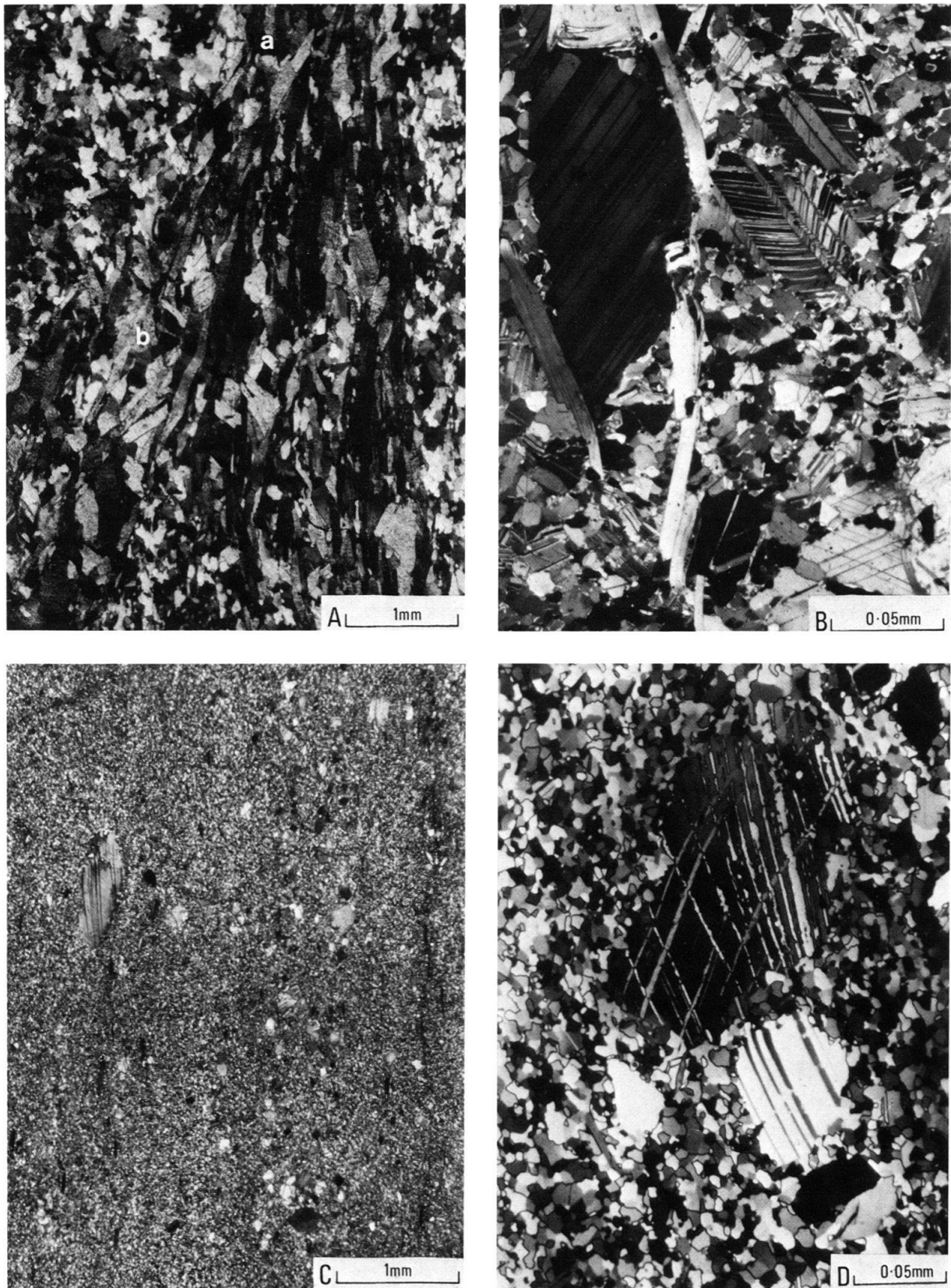


Fig. 18. Microstructures (explanations see opposite page).

### Relationship of Theodul–Rothorn Zone to Mischabel backfold

BEARTH (1953, 1964) has shown that the continuation of the quartzites and carbonate units mapped at the base of the Theodul–Rothorn Zone wedge out parallel to the lower limb of the Mischabel backfold (see Fig. 2). The overall sense of vergence of the  $F_2$  folds within the zone of Mesozoic sediments is consistent for the location of this zone on the lower limb of a major south-east closing fold structure such as the Mischabel backfold. An examination of the shape of  $F_2$  folds from within this zone suggests that extensive shear strain parallel to the boundaries of this zone probably accompanied the  $F_2$  deformation events, and it is this deformation phase that is responsible for the Mischabel backfold, these would be similar to the flexural-slip thrusts described by RAMSAY (1967, p. 395). It would therefore represent a plane of subhorizontal movement that predates many of the vertically oriented  $F_3$  deformation features.

The calcite–dolomite marbles observed almost everywhere close to the Bündnerschiefer boundary, the very discontinuous rauhwacke units that are associated with the above unit, the local recognition of similar units adjacent to the boundary with the Zermatt–Saas Zone, may all be associated with a tectonic zone developed during the  $F_2$  folding phase. Tectonic contacts related to an early phase of folding have clearly been refolded during later penetrative deformation, as has been demonstrated by many previous workers (GÜLLER 1947, BEARTH 1953). However, these carbonate units and their contacts appear to have only been affected by the  $F_3$  deformation phase and are always subparallel to the axial surfaces of the  $F_2$  structures and zone margins. Nowhere was it observed that these units were folded by the  $F_2$  folds, although examples of other folded calcareous units do exist, such as in the Hubel fold closure.

The characteristics of the calcite–dolomite marbles suggest that they may represent a recrystallized mylonite zone, having many similarities to calcite mylonites, e.g. the Lochseiten limestone in the Helvetic nappe (SCHMID 1975). Both the carbonate mylonites and rauhwackes appear to have possessed higher ductility than the surrounding rocks and could have acted as sufficiently ductile units for gliding of the overlying Mesozoic quartzite and Bündnerschiefer. They appear as late thrust slices associated with the formation of the Mischabel backfold; a similar relationship has also been described by WARRAK (1974) in the French Alps.

### Conclusions

The upper Greenschist facies metamorphism seen in the portion of the Combin Zone studied is a direct contrast to the polymetamorphic phases recognized in the underlying Zermatt–Saas Zone. Although many structures recognized in the Combin Zone and Zermatt–Saas Zone (CHADWICK 1974) appear to be similar, they may not correlate as distinct  $F_1$  and  $F_2$  phases, there would probably be an older set of structures in the Zermatt–Saas Zone. No evidence for an unconformity across the Combin Zone and Zermatt–Saas Zone boundary could be established. Instead this boundary is believed to be tectonic in origin with the initial emplacement of the Combin Zone being contemporaneous with the deformation described here as  $F_1$ .

and the associated upper Greenschist facies metamorphism. If thrusting along this boundary had been pre- $F_1$  then this boundary would be deformed by the folding described here as  $F_1$ , no evidence for this could be established in this study.

The  $F_1$  deformation transposed the compositional layering, in the Combin Zone, into orientations subparallel to the top of the Zermatt-Saas Zone. This was followed by the  $F_2$  deformation with the resulting rotation of the units into a series of asymmetric folds that may be regarded as cogenetic with the formation of the Mischabel backfold by reason of their style and orientation. This deformation was also accompanied by further localized thrusting of the Combin Zone over the Zermatt-Saas Zone in narrow shear zones. This is particularly obvious at the base of the quartzite-marble and Bündnerschiefer sequences, where there are minor variations of orientations across these zones. The direction of movement derived from the asymmetry of the  $F_2$  folds may be same as the thrusting movement, that is to the north. The consistent orientation of the  $F_1$  structures as well as the uniform orientation of the  $F_2$  fold phase between the shear zones suggest that the Combin Zone did not undergo major internal disruption during  $F_2$  thrusting. However, there are significant variations in the strain and style of the  $F_2$  deformation which have been attributed to initial compositional differences coupled with a change in deformation path. Similarly  $F_2$  shear zones described here appear to be confined to the overturned (south facing) limb of the large scale Mischabel backfold. Small faults joints and kink bands overprint these structures and may represent either an unloading effect well after the formation of the Mischabel backfold or may be related to differential uplift.

### Acknowledgments

This project was begun while the author was at the Geological Institute Leiden in The Netherlands as a microfabric investigation of the quartzites in a geologically known environment. It soon became obvious that such an investigation couldn't be undertaken without some feel for the structure in the region. Hence it was decided to undertake this study; to this end I would like to thank Professor H. J. Zwart for his encouragement and introducing me to the Mischabel-Rückfalte, and the University of Melbourne for the award of a Travel Grant in order to complete the field work. This work has also been supported by the Australian Research Grants Committee.

### REFERENCES

- ARGAND, E. (1909): *L'exploration géologique des Alpes Pennines centrales*. – Bull. Soc. vaud. Sci. nat. 45/166.
- (1911): *Les nappes de recouvrement des Alpes Pennines et leurs prolongements structuraux*. – Matér. Carte géol. Suisse [n.s.] 31.
- ASHBY, M. F., & VERRALL, R. A. (1973): *Diffusion-accommodated flow and superplasticity*. – Acta metall. 21, 149–163.
- AYRTON, S. N., & RAMSAY, J. G. (1974): *Tectonic and Metamorphic events in the Alps*. – Schweiz. mineral. petrogr. Mitt. 54, 609–639.
- BATHURST, R. G. C. (1971): *Carbonate sediments and their diagenesis*. – Elsevier, Amsterdam.
- BEARTH, P. (1953): *Geologischer Atlas der Schweiz 1:25000, Blatt Zermatt* (Erläuterungen 1953). – Schweiz. geol. Komm.
- (1962): *Versuch einer Gliederung alpinmetamorpher Serien der Westalpen*. – Schweiz. mineral. petrogr. Mitt. 42, 127–137.



- (1964): *Geologischer Atlas der Schweiz 1:25000, Blatt Randa* (Erläuterungen 1964). – Schweiz. geol. Komm.
- (1967a): *Die Ophiolithe der Zone von Zermatt–Saas Fee*. – Beitr. geol. Karte Schweiz [N.F.] 132.
- (1967b): *Visp–St. Niklaus–Zermatt–Gornergrat* (Exkursion Nr. 10). – Geol. Führer Schweiz. Fasc. 3, 146–157 (Wepf, Basel).
- (1975): *Zur Tektonik der Ossola- und Simplon-Region*. – Eclogae geol. Helv. 67, 509–513.
- (1976): *Zur Gliederung der Bündnerschiefer in der Region von Zermatt*. – Eclogae geol. Helv. 69, 149–161.
- BOCQUET, J., DELALOYE, M., HUNZIKER, J.C., & KRUMMENACHER, D. (1974): *K–Ar and Rb–Sr dating of blue amphiboles, micas and associated minerals from the Western Alps*. – Contr. Mineral. Petrol. 47, 7–26.
- CARRARO, F., DAL PIAZ, G.V., & SACCHI, R. (1970): *Serie di Valpelline e II Zona Diorito-kinzigitica sono i relitti di un recoprimento proveniente della Zona Ivrea-Verbano*. – Mem. Soc. geol. ital. 9, 197–224.
- CARRERAS, J., ESTRADA, A., & WHITE, S. (1977): *The effect of folding on the c-axis fabrics of a quartz mylonite*. – Tectonophysics 39, 3–24.
- CHADWICK, B. (1974): *Glaucophane Fabric in the cover of the Monte Rosa Nappe, Zermatt–Saas Fee, Southwest Switzerland*. – Bull. geol. Soc. Amer. 85, 907–910.
- COBBOLD, P.R., COSGROVE, J.W., & SUMMERS, J.M. (1971): *Development of internal structures in deformed anisotropic rocks*. – Tectonophysics 12, 23–53.
- COMPAGNONI, R., DAL PIAZ, G.V., HUNZIKER, J.C., GOSSO, G., LOMBARDO, B., & WILLIAMS, P.F. (1977): *The Sesia–Lanzo zone, a slice of continental crust with Alpine high pressure–low temperature assemblages in the western Italian Alps*. – Rend. Soc. ital. Mineral. Petrol. 33, 281–334.
- COSGROVE, J.W. (1976): *The formation of crenulation cleavage*. – J. geol. Soc. London 132, 155–178.
- DAL PIAZ, G.V., HUNZIKER, J.C., & MARTINOTTI, G. (1972): *La Zona Sesia–Lanzo e l'evoluzione tettonico-metamorfica delle Alpi nordoccidentali interne*. – Mem. Soc. geol. ital. 11, 433–460.
- DAL PIAZ, G.V., & NERVO, R. (1971): *Il lembo di ricoprimento del Glacier–Rafray (Dent Blanche l.s.)*. – Boll. Soc. geol. ital. 90, 401–414.
- DAL PIAZ, G.V., VECCHI, G. DE, & HUNZIKER, J.C. (1977): *The Austroalpine layered gabbros of the Matterhorn and Mt. Collon–Dents de Bertol*. – Schweiz. mineral. petrogr. Mitt. 57, 59–88.
- DICKSON, J.A.D. (1965): *A modified staining technique for carbonates in thin section*. – Nature 4971, 587.
- ELLIOTT, D. (1968): *Interpretation of fold geometry from isogonic maps*. – J. Geol. 76, 171–190.
- FREY, M., HUNZIKER, J.C., FRANK, W., BOCQUET, J., DAL PIAZ, G.V., JÄGER, E., & NIGGLI, E. (1974): *Alpine metamorphism of the Alps, a review*. – Schweiz. mineral. petrogr. Mitt. 54, 247–290.
- GÜLLER, A. (1947): *Zur Geologie der südlichen Mischabel- und Monte Rosa-Gruppe*. – Eclogae geol. Helv. 40, 39–161.
- HEIM, A. (1921): *Geologie der Schweiz* (Bd. 2). – Tauchnitz, Leipzig.
- HOBBS, B.E. (1971): *The analysis of strain in folded layers*. – Tectonophysics 11, 329–375.
- HUDDLESTON, P.J. (1973a): *Fold morphology and some genetic implications of fold development*. – Tectonophysics 16, 1–46.
- (1973b): *The analysis and interpretation of minor folds developed in the Moine rocks of Monar Scotland*. – Tectonophysics 17, 89–132.
- HUDDLESTON, P.J., & STEPHANSSON, O. (1973): *Layer shortening and fold-shape development in the buckling of single layers*. – Tectonophysics 17, 299–321.
- KERRICH, R., FYFE, W.S., GORMAN, B.E., & ALLISON, I. (1977): *Local modification of rock chemistry by deformation*. – Contr. Mineral. Petrol. 65, 183–190.
- KIENAST, J.R. (1973): *Sur l'existence de deux séries différentes au sein de l'ensemble «schistes lustrés–ophiolites» du Val d'Aoste, quelques arguments fondés sur l'étude des roches métamorphiques*. – C.R. Acad. Sci. Paris (D), 276, 2621–2624.
- LEINE, L. (1968): *Rauhwackes in the Cordilleras (Spain). Nomenclature, description and genesis of weathered carbonate breccias of tectonic origin*. – Thesis, Amsterdam.
- MILNES, A.G. (1974): *Structure of the Pennine Zone (Central Alps): A new working hypothesis*. – Bull. geol. Soc. Amer. 85, 1727–1732.
- MISCH, P. (1969): *Paracrystalline microboudinage of zoned grains and other criteria for synkinematic growth of metamorphic minerals*. – Amer. J. Sci. 267, 43–63.
- NAHA, K., & HALYBURTON, R.G. (1977): *Structural pattern and strain history of a superposed fold system in the Precambrian of central Rajasthan India. II.: Strain history*. – Precambrian Res. 4, 85–111.

- RAMSAY, J.G. (1956): *The supposed Moinian basal conglomerate at Glen Strathfarrar, Inverness-shire*. – Geol. Mag. 93, 32–40.
- (1967): *Folding and fracturing of rocks*. – McGraw-Hill, New York.
- ROPER, P.J. (1972): *Structural significance of “Button” or “Fish Scale” texture in phyllonitic schist of the Brevard Zone, North Western South Carolina*. – Bull. geol. Soc. Amer. 83, 853–860.
- RUTLAND, R.W.R. (1965): *Tectonic overpressures*. In: PITCHER, W.S., & FLINN, G.W.: (Eds.): *Controls of Metamorphism* (p. 119–139). – Oliver & Boyd, London.
- SASSI, F.P. (1972): *The petrological and geological significance of the  $b_0$  values of potassic white micas in low-grade metamorphic rocks. An application to the Eastern Alps*. – Tschermin. mineral. petrogr. Mitt. 18, 105–113.
- SCHMID, S.M. (1975): *The Glarus Overthrust: Field evidence and mechanical model*. – Eclogae geol. Helv. 68, 247–280.
- SCHMID, S.M., BOLAND, J.N., & PATERSON, M.S. (1977): *Superplastic flow in finegrained limestone*. – Tectonophysics 43, 257–291.
- WARRAK, M. (1974): *The petrography and origin of dedolomitized, veined or brecciated carbonate rocks, the “Cornieules”, in the Fréjus region, French Alps*. – J. geol. Soc. London 130, 229–247.
- WHITE, S. (1976): *The effects of strain on the microstructures, fabrics and deformation mechanisms in quartzites*. – Phil. Trans. r. Soc. London (A), 283, 69–86.
- WILSON, C.J.L. (1977): *Combined diffusion-infiltration of Uranium in micaceous schists, a study using the fission track method*. – Contr. Mineral. Petrol. 65, 171–181.
- (1978): *Development of schistosity in phengite schists from Zermatt Switzerland – a discussion*. – Tectonophysics (in press).

